NASA
Technical
Paper
2537

January 1986

The Application to Airfoils of a Technique for Reducing Orifice-Induced Pressure Error at High Reynolds Numbers

E. B. Plentovich

NASA

NASA Technical Paper 2537

1986

The Application to Airfoils of a Technique for Reducing Orifice-Induced Pressure Error at High Reynolds Numbers

E. B. Plentovich

Langley Research Center
Hampton, Virginia

National Aeronautics and Space Administration

Scientific and Technical Information Branch

SUMMARY

A wind-tunnel investigation was conducted in the Langley 0.3-Meter Transonic Cryogenic Tunnel to study the effects of porous (sintered metal) plug orifices on orifice-induced static-pressure measurement error at high Reynolds numbers. An NACA 65_1-213 airfoil was tested at Mach numbers from 0.60 to 0.80 and at Reynolds numbers from 6×10^6 to 40×10^6. Data are included which compare pressure measurements obtained from porous plug orifices and from conventional orifices with diameters of 0.025 cm (0.010 in.) and 0.102 cm (0.040 in.). The two-dimensional airfoil code GRUMFOIL was used to calculate boundary-layer displacement thickness. The response time and the downstream effect of the porous plug orifice were considered in this investigation. The results showed that the porous plug orifice could be a viable method of reducing pressure error. The data also showed that the pressure measurements obtained with a 0.102-cm-diameter orifice were very close to the measurements obtained with a 0.025-cm-diameter orifice over much of the airfoil and that downstream of a shock the orifice size was not critical.

INTRODUCTION

In the past, many experiments have been conducted to study orifice-induced static-pressure measurement error (e.g., refs. 1-8). Recently, interest in this work has arisen again because of the construction of high Reynolds number facilities. Previous work on the subject of orifice-induced pressure measurement error has led to the conclusion that there are three main mechanisms by which a conventional orifice in subsonic flow can induce an error in the static-pressure measurement (ref. 1). These mechanisms are (1) the flow deflecting into the orifice, (2) an eddy or system of eddies forming within the orifice, and (3) the pitot effect whereby the flow stagnates at the downstream edge of the orifice. These phenomena combine to produce a measured pressure which is too high. The magnitude of this error is influenced by the following geometric factors: the ratio of the hole diameter to the hole depth; the inclination of the hole axis relative to the surface; and the condition of the hole entry with respect to roundness, burrs, and chamfer.

In most wind tunnels, the boundary-layer displacement thickness, δ^*, is generally large compared with the orifice diameter, d. At moderate Reynolds numbers, the orifice has little effect on the boundary layer, and it has been found that the orifice-induced pressure measurement error can be considered negligible. In a high Reynolds number facility, δ^* can be up to an order of magnitude thinner, so the orifice will most likely have a larger effect on the boundary layer. Most previous work on orifice-induced static-pressure measurement error was conducted at subsonic flow conditions for which the ratio of d/δ^* was less than 4, values typical of a conventional subsonic wind tunnel.

To determine if there was a measurable orifice-induced pressure measurement error at high Reynolds numbers, an investigation was conducted in the Langley 7- by 10-Foot High-Speed Tunnel (7 × 10 HST) (ref. 9). A flat plate was used to test orifices which were scaled models several times the size of conventional orifices. Though the test was conducted at moderate Reynolds numbers, orifice diameter was used to increase the values of d/δ^* to simulate high Reynolds number flow. During the test, a piece of sintered (porous) metal was installed flush with the model surface.

The porous metal was employed in an attempt to eliminate the mechanisms, stated above, which cause orifice-induced pressure measurement error and thereby reduce the error to a negligible amount. The data showed that on a flat plate in a zero or slightly adverse pressure gradient, there was measurable error which increased as orifice diameter increased. However, for the orifice with the porous metal plug, the error associated with the same size conventional orifice was virtually eliminated.

Because the porous plug orifices had provided such favorable results, the concept was further studied in the Langley 0.3-Meter Transonic Cryogenic Tunnel (0.3-m TCT) at high Reynolds numbers, and the results are described herein. An NACA 65_1-213 airfoil was tested in the 0.3-m TCT at Mach numbers of 0.60 to 0.80 and at Reynolds numbers (based on the chord) from 6×10^6 to 40×10^6. Pressure measurements were made to compare porous plug orifices with conventional orifices having two diameters, 0.102 cm (0.040 in.) and 0.025 cm (0.010 in.).

SYMBOLS AND ABBREVIATIONS

b	model span or tunnel width, cm
c	model chord, cm
c_d	section drag coefficient
c_l	section lift coefficient
c_n	section normal-force coefficient
C_p	pressure coefficient
C_p^*	pressure coefficient corresponding to sonic speed
d	diameter of static-pressure orifice, cm
H	shape factor, δ^*/θ
ID	inner diameter
LN_2	liquid nitrogen
M_∞	free-stream Mach number
R_c	Reynolds number based on model chord
RMS	root-mean-square
t	time, sec
x	chordwise distance measured from leading edge of airfoil, cm
y	spanwise distance measured from left side of airfoil, cm
z	vertical distance measured from chord line of airfoil, cm
α	angle of attack, deg

$\bar{\beta}$ defined in equation (4)

δ^* boundary-layer displacement thickness, cm

η $y/(b/2)$

θ boundary-layer momentum thickness, cm

WIND-TUNNEL DESCRIPTION

The NACA 65_1-213 airfoil model was tested in the 20- × 60-cm two-dimensional test section of the 0.3-m TCT. A photograph of the tunnel is shown in figure 1(a), and a schematic drawing showing some physical characteristics of the tunnel is shown in figure 1(b). Figure 2 is a photograph showing the model installed in the 20- × 60-cm two-dimensional test section. In the photograph, the plenum lid and test-section ceiling have been removed to show model installation. This tunnel is a continuous flow, fan-driven, transonic tunnel which uses nitrogen gas as the test medium. It is capable of operating at temperatures varying from about 80 K (-316°F) to about 327 K (129°F) and stagnation pressures ranging from slightly greater than 1 atm to 6 atm (1 atm = 101.325 kPa). Test-section Mach number can be varied from about 0.20 to 0.85. The ability to operate at cryogenic temperatures and moderately high total pressure provides a very high Reynolds number capability at model loadings which are low relative to those at which the same Reynolds number is obtained at ambient temperatures and very high total pressure. More detailed operational information can be found in references 10, 11, and 12.

MODEL DESCRIPTION

Figure 3 shows a schematic drawing of the NACA 65_1-213 airfoil model used in this investigation. This two-dimensional pressure model has a chord of 15.24 cm (6.00 in.), a span of 20.17 cm (7.94 in.), and static-pressure orifices located only on the upper surface. The model was constructed from a high-strength steel alloy, and the fabrication tolerance of the model coordinates was within ±0.005 cm (0.002 in.). The surface finish on the upper surface of the model was specified to be 0.4 μm (16×10^{-6} in.) RMS, and on the lower surface 0.8 μm (32×10^{-6} in.) RMS.

For the first tunnel entry, the orifices were located as shown in figure 4(a). Three chordwise rows of static-pressure orifices were installed near the midspan. Porous (sintered metal) plug orifices were installed on the centerline with 0.025-cm-diameter (0.010-in.) and 0.102-cm-diameter (0.040-in.) orifices to either side. The 0.025-cm-diameter orifice was chosen because it is the standard orifice size used in models tested in the 0.3-m TCT. This orifice is considered to provide "correct" measurements and was used as the standard for comparison purposes. The 0.102-cm-diameter conventional orifice was sized to match the 0.102-cm diameter of the porous plugs. There were also three spanwise rows of 0.025-cm-diameter orifices (see fig. 4(a)) to investigate the two-dimensionality of the flow over the airfoil. Nine 0.025-cm-diameter orifices were grouped near the leading edge to study the downstream effects of the porous plug orifice.

The initial installation of porous plug orifices was made by diffusion bonding the porous metal in the end of a type 347 stainless steel tube which had an inner diameter of 0.102 cm (0.040 in.) and an outer diameter of 0.152 cm (0.060 in.). The tube was then attached to the model with an adhesive. A sketch of the method of

installation is shown in figure 4(b). To keep the thermal properties of the pieces as similar as possible, type 347 stainless steel was also used to manufacture the sintered metal for the porous plug. The porous plug was specified to be 0.160-cm (0.063-in.) thick with a filtration rating of 20 μm (7.9×10^{-4} in.) and to be installed flush with the end of the tubing. (The filtration rating specifies the size of a contaminant particle which would be retained by the porous metal and is used herein to identify the material.) Figure 5 is a close-up of the model upper surface showing the porous plug orifices installed in the airfoil.

The original method of installation did not keep the porous plug orifices flush with the model surface during cryogenic testing; therefore, the model was modified slightly as shown in figure 6(a) for the second tunnel entry. Eight of the 0.102-cm-diameter (0.040-in.) conventional orifices were filled with cryogenic structural adhesive and were sanded smooth with the model surface. The remaining five 0.102-cm-diameter holes near the leading edge (see fig. 6(a)), were used to test a new method of installing porous metal into orifices, which is sketched in figure 6(b). For the new method of installation, the porous plugs were cut from type 316 stainless steel sintered metal which had a filtration rating of 20 μm. Type 316 stainless steel was used instead of type 347 stainless steel because the coefficients of expansion were nearly the same, and type 316 stainless steel was readily available. The plugs were cut on a slight taper, with the largest part of the taper being slightly larger than the hole diameter, and were pressed into the holes by hand. The plugs were then lightly filed to make them flush with the model surface.

TEST DESCRIPTION

The model was tested in the 0.3-m TCT at Mach numbers from 0.60 to 0.80 and at Reynolds numbers (based on the chord) from 6×10^6 to 40×10^6 over an angle-of-attack range of -1° to 3°. The Reynolds number and Mach number ranges used in these test programs are shown in figure 7. Prior to data being taken, the model was allowed to reach thermal equilibrium. All runs were made with boundary-layer transition location unfixed. Though the transition location was not fixed, based on previous experience it was estimated that the airfoil transitioned before 10 percent of the chord. The flow was expected to have transitioned by this point because of high noise levels in the 0.3-m TCT (ref. 13), and because orifices tend to disturb the flow locally and induce turbulent flow over all downstream orifices (ref. 14).

DISCUSSION OF RESULTS

Repeatability

To insure the consistency of the wind-tunnel results, repeat data were taken for each angle-of-attack sweep, and a few repeat data points were taken at the end of the test for comparison with data obtained at the beginning of the test. Figures 8 through 11 are typical for each type of repeat data. Repeat data comparing tunnel entries are also shown in figure 12. The variations in data between tunnel entries could be attributed to a slight difference in angle of attack induced by the minor tunnel geometry changes at different temperatures.

Two-Dimensionality of Flow

To study the two-dimensionality of the flow over the NACA 65_1-213 model, three spanwise rows of orifices were located on the model. These were placed at x/c locations of 0.138, 0.417, and 0.790. Shown in figures 13 and 14 are representative samples of the pressures measured at these spanwise rows for both tunnel entries. It can be seen from these figures that the flow near the centerline of the model can be considered two-dimensional.

Effect on Orifices Downstream

Near the leading edge of the model were nine 0.025-cm-diameter (0.010 in.) orifices, as shown in figure 4(a). During the first tunnel entry, these orifices were used to determine if the porous plug orifice had an effect on downstream pressure measurements. The measurements behind the porous plug orifice were compared with measurements obtained from orifices which had been placed where no upstream orifices would influence their measurements and with measurements from orifices downstream of a 0.025-cm orifice. If the porous plug orifice had influenced the downstream orifices, it would have been evidenced by a difference in the pressures measured by the orifices directly downstream of the porous plug orifices as compared with the others. Representative samples of the pressures measured by these orifices are shown in figure 15. The 0.025-cm orifices immediately upstream and downstream of the group of nine orifices are shown to provide a reference for the magnitude of the pressure in that region. As can be seen from the figure, the pressures measured by the orifices downstream of the porous plug orifices do not seem to be affected any more than the pressures measured downstream of the 0.025-cm orifices or those measured in the region unaffected by upstream orifices.

Orifice Response Times

The response times of the porous plug orifices used in the model were studied prior to testing. The response time of the tubes was measured by connecting the open end of the tube containing the porous plug to a pressure of 0.68 atm (10 psig) while the porous plug end was tightly sealed. With this arrangement, when the seal was removed from the porous plug end, the time required for the orifice to leak from 0.68 atm to 0 atm (0 psig) could be determined and was considered to be the response time. For the porous plug orifices tested in this model, the length of time required varied from 6 to 20 sec, depending on the porosity of the material (the percentage of void volume within the structure) and the thickness of the porous plug. (Though the porosity and thickness of the porous material were specified to be the same for all plugs, there were slight differences which had no impact on the static-pressure measurement.) For a conventional orifice, which is basically an open hole, the major factors relating to the reponse time are the orifice diameter, the tube diameter, the transducer volume, and the length of the tubing connecting the orifice to the transducer. The response time for a conventional 0.025-cm-diameter (0.010-in.) orifice is about 5 sec. However, for a porous plug orifice, the increased response time would be caused by the restriction at the surface.

The first run of the test was used to determine the necessary delay time once the tunnel had been stabilized at the specified conditions, before steady pressure data could be taken. To do this, the signals from four orifices, a 0.025-cm-diameter (0.010-in.) orifice and a porous plug orifice at $x/c = 0.025$ and a 0.025-cm-diameter (0.010-in.) orifice and a porous plug orifice at $x/c = 0.417$, were

connected to an oscillograph, which provided traces of the measured pressures. Figure 16 shows a sample of these results from a run made at $M_\infty = 0.60$ and $R_c = 15 \times 10^6$. The time scale is provided as a point of reference. At the beginning of this run, $t = 0$ sec, the tunnel conditions were being held constant. Just before $t = 10$ sec, the angle of attack of the model was increased by 1°. From figure 16, it can be seen that it takes about 40 sec for the pressure measurements to stabilize again. Though this appears to be a considerably longer period of time than the response time previously stated, it should be noted that this length of time also included the time necessary to stabilize the tunnel conditions after the change in α of 1°.

The second method used to study response time during the test was to obtain data points at several time intervals after tunnel conditions were stabilized. The tunnel conditions were achieved and stabilized as rapidly as possible, then a data point was immediately taken ($t = 0$ sec). Data were then taken at $t = 10$ sec, $t = 20$ sec, $t = 30$ sec, and $t = 50$ sec. As can be seen in figure 17, once the tunnel conditions had been stabilized, the pressure measurements on the model had also stabilized. Therefore, data could be taken immediately after achieving the desired test conditions, even with the porous plug orifices.

Pressure Distributions

Shown in figures 18 and 19 are representative pressure distributions obtained on the NACA 65_1-213 airfoil during the first tunnel entry. Each plot shows the pressure distribution measured by the three chordwise rows of orifices: the porous plug orifices, the 0.025-cm-diameter (0.010-in.) orifices, and the 0.102-cm-diameter (0.040-in.) orifices. The pressures shown in figures 18 and 19 are the measured pressures and have not been corrected for sidewall or top and bottom wall interference.

In planning for this test, the 0.025-cm-diameter (0.010-in.) orifices were chosen to provide the "reference" measurements. Based on the results obtained in the previously mentioned flat plate study in the 7 × 10 HST (ref. 9), the 0.102-cm-diameter (0.040-in.) orifices were chosen because it was thought they would provide pressure measurements that were very much in error because of the large hole diameter compared with the boundary-layer displacement thickness. From the previous test in the 7 × 10 HST (ref. 9), it was expected that the porous plug orifices would provide a pressure measurement that was less in error (a more negative pressure measurement) than even the 0.025-cm orifices. The results in figures 18 and 19 show that this did not happen. With measurements from the 0.025-cm orifices as the "reference," near the leading edge, measurements from the 0.102-cm orifices seem to be only slightly in error (more positive C_p values), whereas measurements from the porous plug orifices have more error. The porous plug orifice pressure measurements were in error because of problems with the method of installation, which were discussed in the section on model description. Moving toward the trailing edge, these differences lessen. In fact, beyond 30 percent of the chord, the measurements obtained from the 0.025-cm orifices and the 0.102-cm orifices are very nearly the same, while the porous plug orifice measurements are still in error. Near the trailing edge of the airfoil or downstream of the shock, where the boundary layer has thickened considerably, the size of the orifice does not seem to be a concern, as all orifices provide approximately the same pressure measurement.

The agreement between the 0.102-cm (0.040-in.) orifices and the 0.025-cm (0.010-in.) orifices is quite surprising and was not expected based on previous

research (refs. 2, 6, and 9). However, the results obtained in the other investigations were from zero or slightly adverse pressure gradient flows on a model with no streamwise curvature, whereas the results from this investigation were obtained on an airfoil for which initially there was a highly favorable pressure gradient. The model curvature or the favorable pressure gradient at the leading edge could have been a factor in reducing the expected induced error associated with the 0.102-cm orifice.

Shown in figures 20 and 21 are pressure distributions from the second entry. In the region very near the leading edge (up to about $x/c = 0.1$), where the boundary layer is very thin, the newly installed porous plug orifices seem to provide a more accurate measurement, or a more negative value of C_p, than the 0.025-cm (0.010-in.) orifices. As the boundary layer thickens, the difference in measurements between the new porous plug orifices and the 0.025-cm orifices lessens until the measurements are the same. Though measurements were obtained from the original porous plug orifices in the second entry, the data are not shown in figures 20 and 21, since the method of installation did not retain the orifices flush with the model surface during cryogenic testing.

Theoretical Comparisons

The GRUMFOIL code (ref. 15) was used to estimate the boundary-layer displacement thickness, δ^*, on the airfoil (fig. 22). To verify the reasonableness of the δ^* calculations, pressure data obtained on the NACA 65_1-213 airfoil in the first entry were compared with calculated theoretical pressure distributions (figs. 23 and 24). The theoretical code GRUMFOIL was used because it is considered "state of the art" for two-dimensional airfoils and would therefore provide the most accurate theoretical results with which the experimental results could be compared. The calculated values were based on an estimated transition location of $x/c = 0.10$.

The comparisons of the corrected experimental data with the theoretical GRUMFOIL results (figs. 23 and 24) show that for the most part, GRUMFOIL does an exceptional job of modeling the flow around a two-dimensional airfoil. The values of δ^* in figure 22 can then be considered reasonable estimates. Based on the calculated δ^* (fig. 22), the values of d/δ^* were found to range from about 20 to 200 near the leading edge. The ratio of d/δ^* decreased to about 0.3 near the model trailing edge. This test did extend the range of d/δ^* beyond values previously available and into the range expected to be seen in high Reynolds number testing.

Only a few test conditions were able to be run with GRUMFOIL because of limitations imposed on the present investigation. Because the NACA 65_1-213 model in this study has orifices only on the upper surface, c_l could not be calculated. Since the wake rake was not installed for this investigation, c_d could not be determined. However, prior to this test, a different NACA 65_1-213 airfoil model had been tested in the 0.3-m TCT (ref. 16). Figure 25 shows a pressure distribution from the previous NACA 65_1-213 airfoil test compared with the pressures measured by the 0.025-cm-diameter (0.010-in.) orifices in the present test. The 0.025-cm orifices were used for the comparison, as the NACA 65_1-213 model from the previous program had orifices which were 0.025 cm in diameter. As can be seen from figure 25, which was representative of all comparisons made, the pressure distributions over the two models agree very well on the upper surface. Because the pressures from the two models matched so well, it was assumed that the c_l values, computed from pressure measurements, and the c_d values calculated from the traversing wake probe on the model in reference 16, could be used for the present NACA 65_1-213 model with the porous plug

orifices. A limited number of runs from the two tests had been made at the same M_∞ and R_c. These runs were used to calculate the values of δ^*.

Since GRUMFOIL generates results for a two-dimensional airfoil in free air, the experimental data (M_∞, C_p, and c_l) were corrected for tunnel wall interference. Reference 17 indicated that the slotted wall in the floor and ceiling of the two-dimensional test section in the 0.3-m TCT had been designed for zero blockage. Reference 18 shows that it is not as critical to correct for the solid blockage effects as it is to correct for sidewall boundary-layer effects in the 0.3-m TCT when the slotted walls are installed for the floor and ceiling. Since the slotted walls were used for the floor and ceiling, the data were only corrected for sidewall interference by the method presented by Sewall in reference 19. This method extends the subsonic similarity rule derived by Barnwell (ref. 20) to transonic conditions. The corrections for free-stream Mach number, pressure coefficient, and section normal-force coefficient, given in reference 19, are as follows:

$$\frac{\bar{\bar{M}}_\infty}{\left(1 - \bar{\bar{M}}_\infty^2\right)^{3/4}} = \frac{M_\infty}{(\bar{\beta})^{3/2}} \tag{1}$$

$$\bar{\bar{C}}_p = \frac{\bar{\beta}}{\left(1 - \bar{\bar{M}}_\infty^2\right)^{1/2}} C_p \tag{2}$$

and

$$\bar{\bar{c}}_n = \frac{\bar{\beta}}{\left(1 - \bar{\bar{M}}_\infty^2\right)^{1/2}} c_n \tag{3}$$

where

$$\bar{\beta} = \left[1 - M_\infty^2 + \frac{2\delta^*}{b}\left(2 + \frac{1}{H} - M_\infty^2\right)\right]^{1/2} \tag{4}$$

The above values which are "double barred" are corrected values, while the unbarred values are uncorrected. Also note that b is the tunnel width.

CONCLUDING REMARKS

With the advent of high Reynolds number facilities, the boundary layer on models tested in these facilities has become much thinner. In the high Reynolds number facilities, a boundary-layer displacement thickness much smaller than the orifice diameter can cause orifice-induced static-pressure measurement error to become a concern once again. A previous investigation in the Langley 7- by 10-Foot High-Speed Tunnel to study the error induced by several orifice sizes showed that the error increased as the ratio of hole diameter to boundary-layer displacement thickness

increased; however, a piece of sintered (porous) metal installed in a large hole reduced the error to a negligible amount.

To further study the porous plug orifices, an experiment was conducted in the Langley 0.3-Meter Transonic Cryogenic Tunnel on a NACA 65_1-213 airfoil at Mach numbers from 0.60 to 0.80 and Reynolds numbers (based on the chord) from 6×10^6 to 40×10^6. Measurements from porous plug orifices were compared with measurements from orifices with diameters of 0.025 cm (0.010 in.) and 0.102 cm (0.040 in.). It was found that if the porous plug was carefully made to be flush with the surface of the model, then the porous plug orifice could be a viable method of reducing orifice-induced static-pressure error. The benefits of the porous plug orifice in reducing orifice-induced static-pressure error are noticeable only on about the first 10 percent of the airfoil chord, after which the difference in static-pressure error between the porous plug orifice and the conventional 0.025-cm-diameter orifice is negligible. The porous plug orifice would also be beneficial in eliminating errors induced by holes that were out-of-round, had burrs, or were chamfered. The orifice-induced pressure error associated with the measurements made by 0.102-cm-diameter orifices was less than expected, even in the leading-edge region. (Possibly the model curvature and/or the favorable pressure gradient could have been a factor in reducing the pressure error.) It appears that downstream of about 30 percent of the chord, an orifice larger than the conventional 0.025-cm-diameter orifice could be used with minimal effect on measured pressure error. Downstream of the shock wave, the boundary layer has thickened and, as was expected, the pressure measurements in this region did not appear to be a function of orifice size over the range of orifices tested.

NASA Langley Research Center
Hampton, VA 23665-5225
November 6, 1985

REFERENCES

1. Shaw, R.: The Influence of Hole Dimensions on Static Pressure Measurements. J. Fluid Mech., vol. 7, pt. 4, Apr. 1960, pp. 550-564.

2. Rainbird, W. J.: Errors in Measurement of Mean Static Pressure of a Moving Fluid Due to Pressure Holes. Nat. Res. Counc. Can. Quart. Bull., no. 3, 1967, pp. 58-89.

3. Franklin, R. E.; and Wallace, James M.: Absolute Measurements of Static-Hole Error Using Flush Transducers. J. Fluid Mech., vol. 42, pt. 1, June 4, 1970, pp. 33-48.

4. Pugh, P. G.; Peto, J. W.; and Ward, L. C.: Experimental Verification of Predicted Static Hole Size Effects on Model With Large Streamwise Pressure Gradients. C.P. No. 1139, British A.R.C., 1971.

5. Ray, A. K.: Einfluss der Bohrlochgrösse auf die Anzeige des statischen Druckes bei verschiedenen Reynoldszahlen (On the Effect of Orifice Size on Static Pressure Reading at Different Reynolds Numbers). Ing.-Arch., Bd. XXIV, Drittes Heft, 1956, pp. 171-181.

6. Rayle, R. E.: Influence of Orifice Geometry on Static Pressure Measurements. ASME Paper No. 59-A-234, Nov.-Dec. 1959.

7. Billington, I. J.: Experimental Assessment of the Validity of Pressure Measurements in the Fluid Film Between Seal Faces. Proceedings of the Second International Conference on Fluid Sealing (Cranfield, England), The British Hydromechanics Research Association, 1964, pp. F3-29 - F3-44.

8. Kuwano, H.; Wu, J. M.; and Moulden, T. H.: An Experimental Study of Orifice Size on Static Pressure Measurements. Proceedings of the Twelfth International Symposium on Space Technology and Science, Hideo Nagasu, ed., AGNE Publ., Inc., 1977, pp. 175-180.

9. Plentovich, E. B.; and Gloss, B. B.: Effects of Reynolds Number on Orifice Induced Pressure Error. AIAA-82-0613, Mar. 1982.

10. Kilgore, Robert A.: Design Features and Operational Characteristics of the Langley 0.3-Meter Transonic Cryogenic Tunnel. NASA TN D-8304, 1976.

11. Ray, Edward J.; Ladson, Charles L.; Adcock, Jerry B.; Lawing, Pierce L.; and Hall, Robert M.: Review of Design and Operational Characteristics of the 0.3-Meter Transonic Cryogenic Tunnel. NASA TM-80123, 1979.

12. Ray, Edward J.: A Review of Reynolds Number Studies Conducted in the Langley 0.3-m Transonic Cryogenic Tunnel. AIAA-82-0941, June 1982.

13. Stainback, P. Calvin; Johnson, Charles B.; and Basnett, Constance B.: Preliminary Measurements of Velocity, Density and Total Temperature Fluctuations in Compressible Subsonic Flow. AIAA 83-0384, Jan. 1983.

14. Somers, Dan M.; Stack, John P.; and Harvey, William D.: Influence of Surface Static-Pressure Orifices on Boundary-Layer Transition. NASA TM-84492, 1982.

15. Melnik, R. E.; Mead, H. R.; and Jameson, A.: A Multi-Grid Method for the Computation of Viscid/Inviscid Interactions on Airfoils. AIAA-83-0234, Jan. 1983.

16. Plentovich, E. B.; Ladson, Charles L.; and Hill, Acquilla S.: Tests of a NACA 65_1-213 Airfoil in the NASA Langley 0.3-Meter Transonic Cryogenic Tunnel. NASA TM-85732, 1984.

17. Barnwell, Richard W.: Design and Performance Evaluation of Slotted Walls for Two-Dimensional Wind Tunnels. NASA TM-78648, 1978.

18. Murthy, A. V.; Johnson, C. B.; Ray, E. J.; Lawing, P. L.; and Thibodeaux, J. J.: Investigation of the Effects of Upstream Sidewall Boundary-Layer Removal on a Supercritical Airfoil. AIAA-83-0386, Jan. 1983.

19. Sewall, W. G.: The Effects of Sidewall Boundary Layers in Two-Dimensional Subsonic and Transonic Wind Tunnels. AIAA-81-1297, June 1981.

20. Barnwell, Richard W.: Similarity Rule for Sidewall Boundary-Layer Effect in Two-Dimensional Wind Tunnels. AIAA Journal, vol. 18, no. 9, Sept. 1980, pp. 1149-1151.

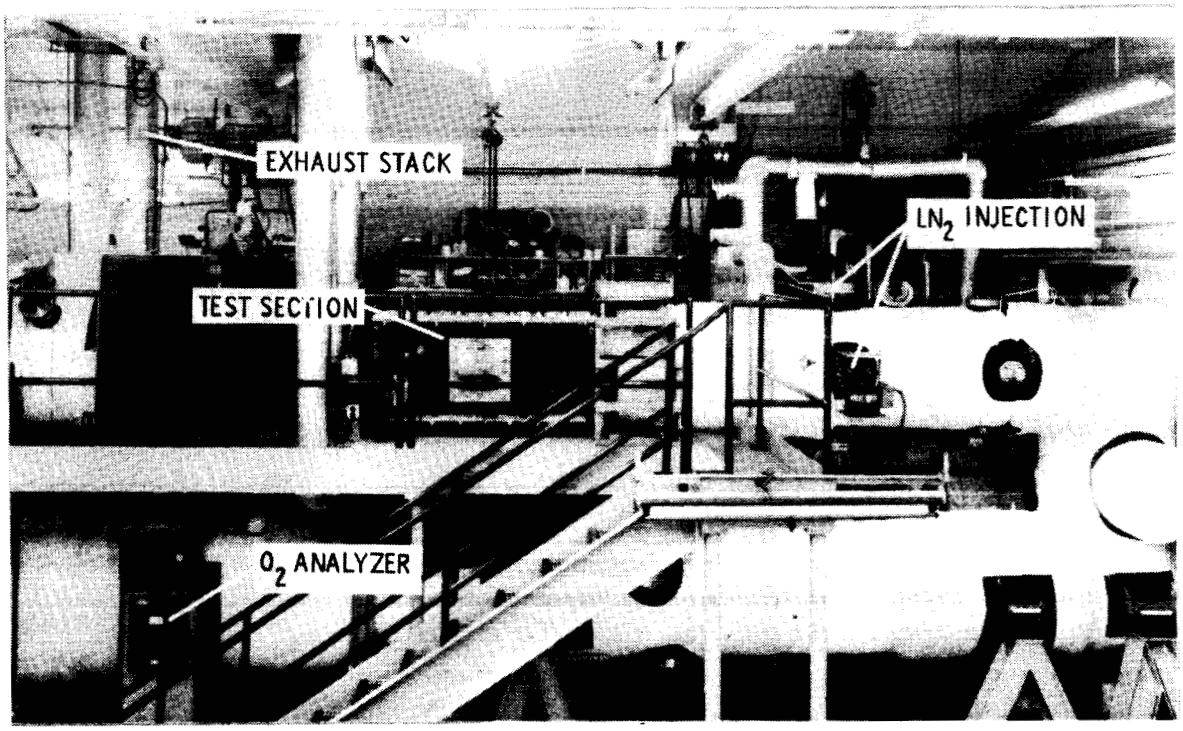

L-79-2147.1

(a) Photograph.

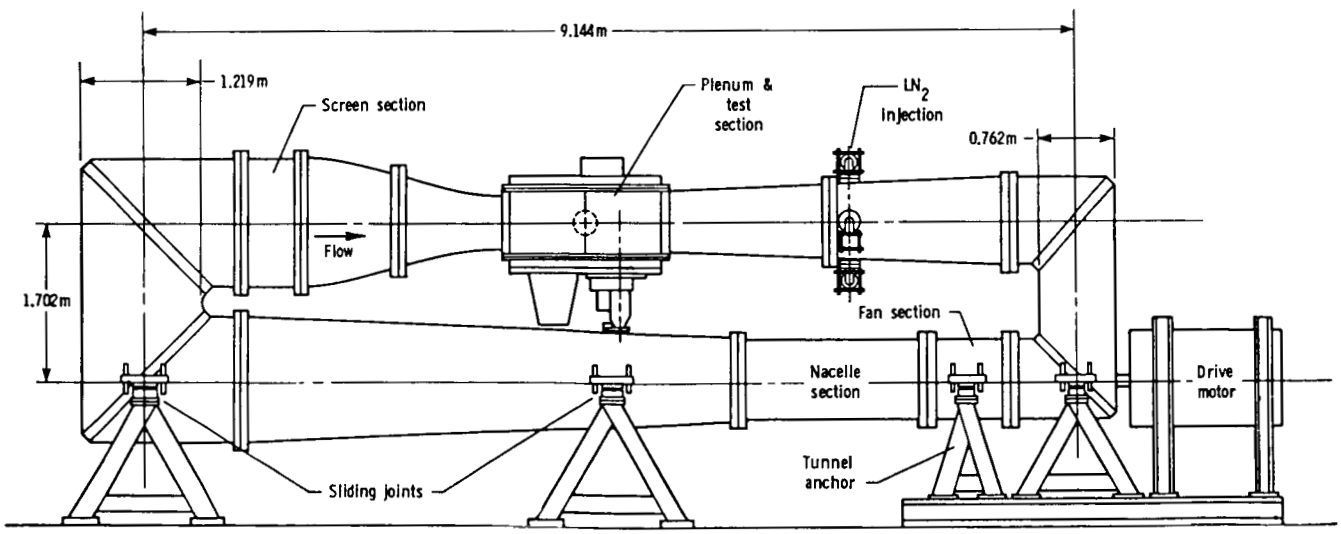

(b) Schematic drawing.

Figure 1.- Elevation view of 0.3-m TCT with two-dimensional test section installed.

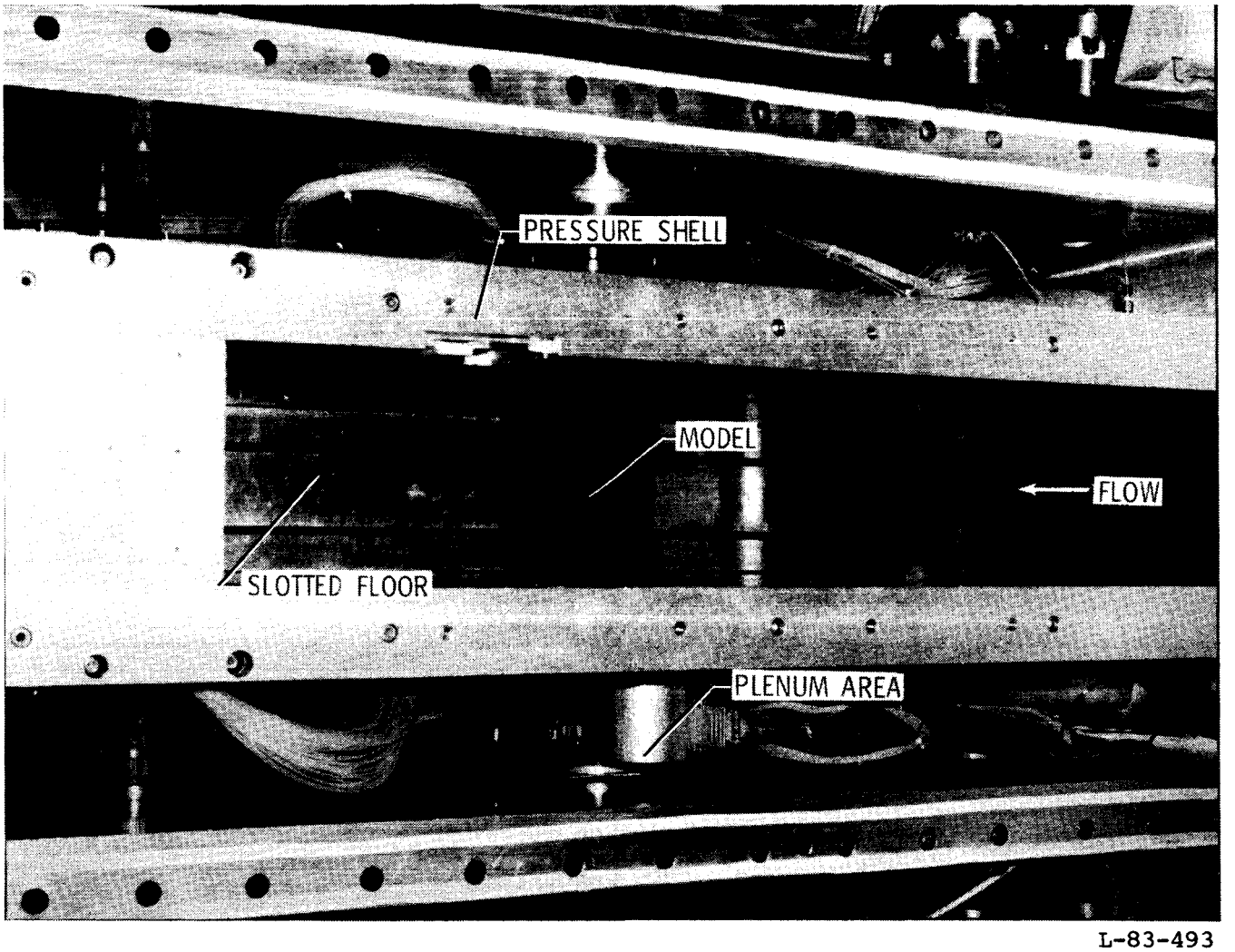

L-83-493

Figure 2.- NACA 65_1-213 model installed in two-dimensional test section of 0.3-m TCT.

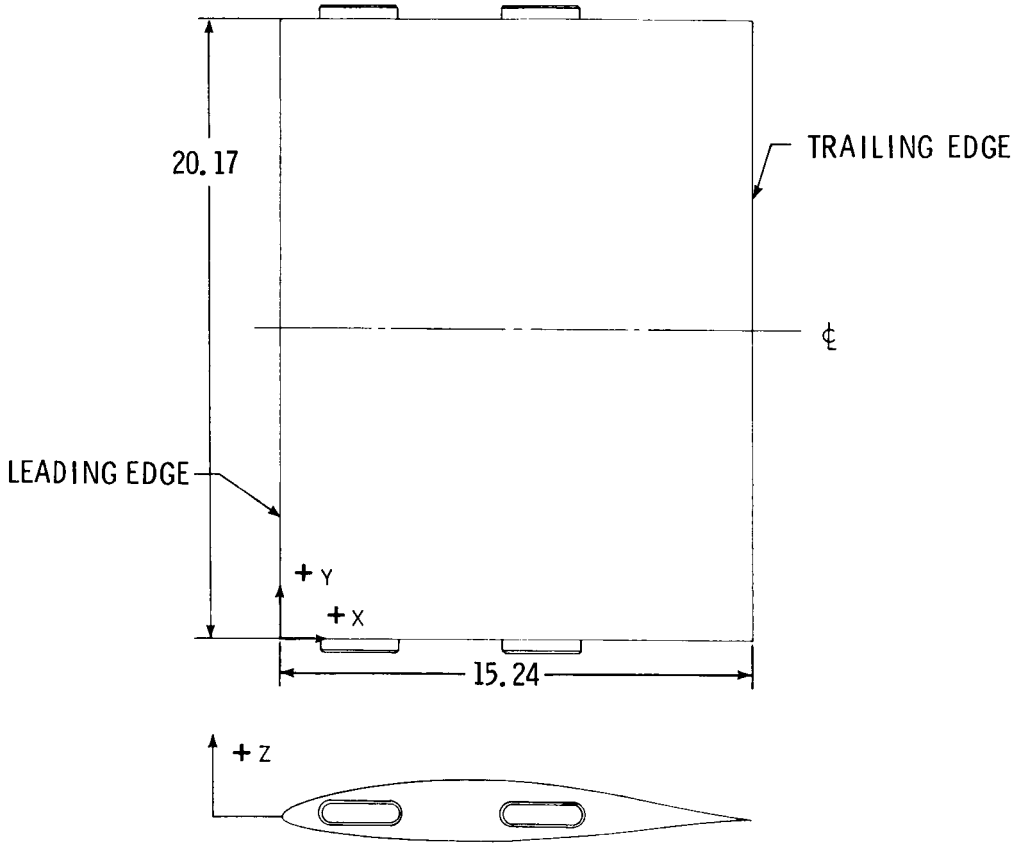

Figure 3.- Schematic drawing of NACA 65_1-213 model.
(All dimensions are in centimeters.)

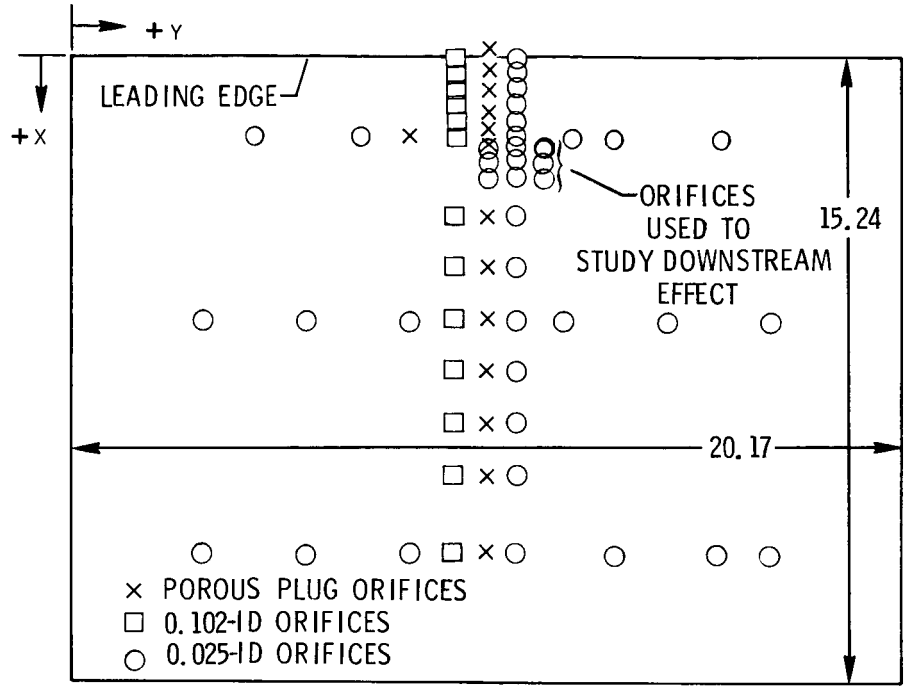

(a) Placement of orifices on upper surface of model. (All dimensions are in centimeters.)

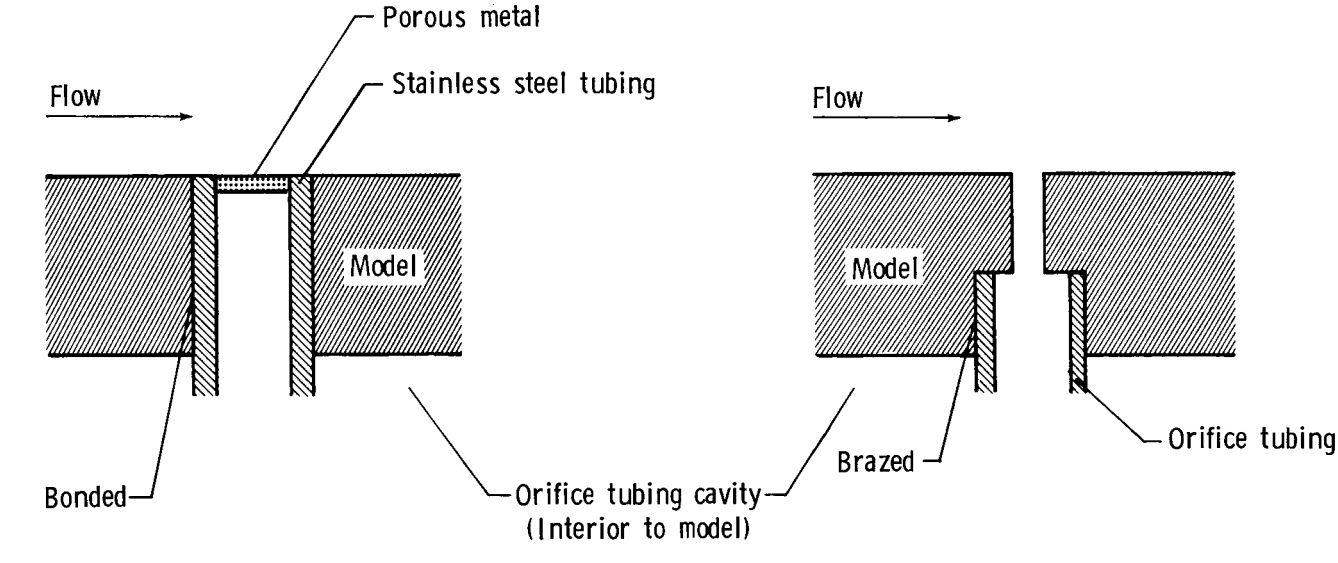

(b) Cross section of orifice construction (not drawn to scale).

Figure 4.- Model construction for first tunnel entry.

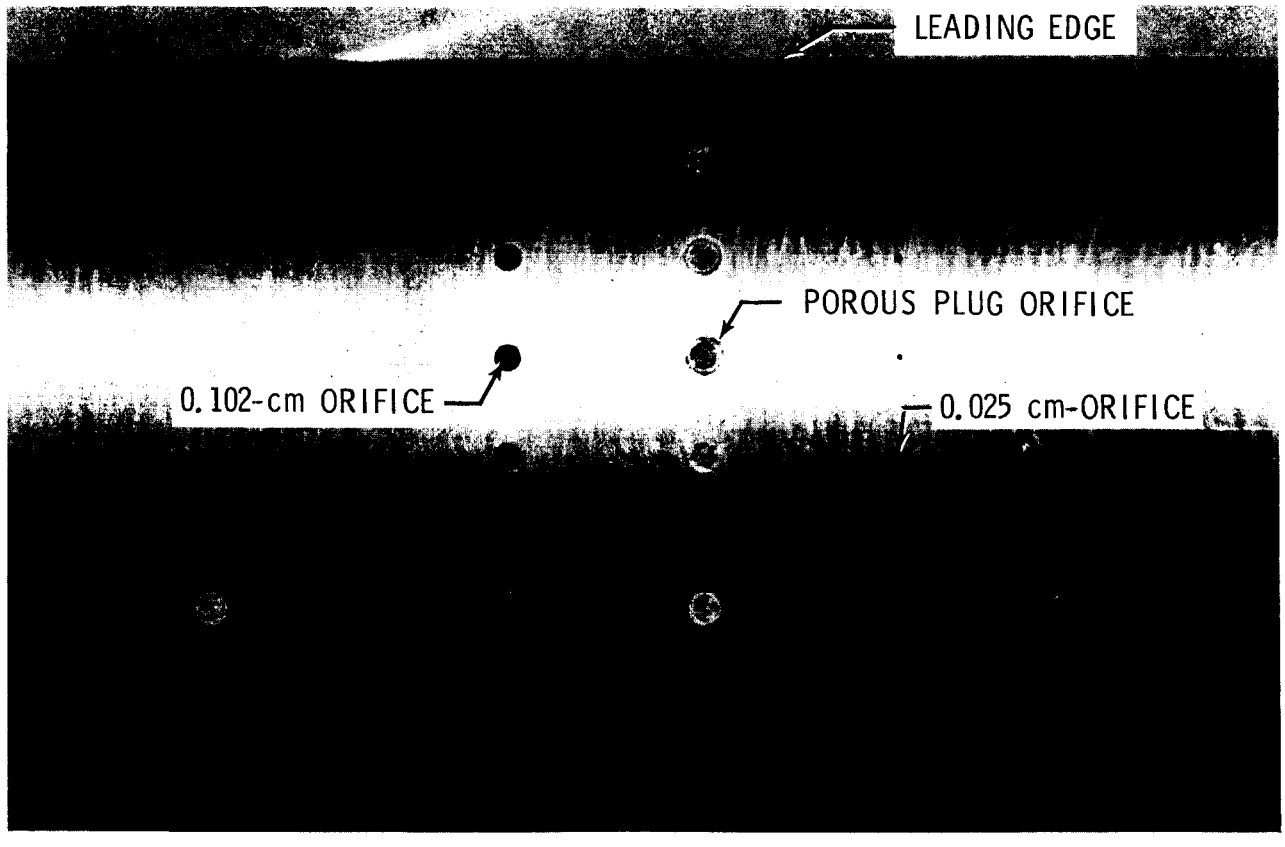

L-85-156

Figure 5.- Close-up of upper surface of model.

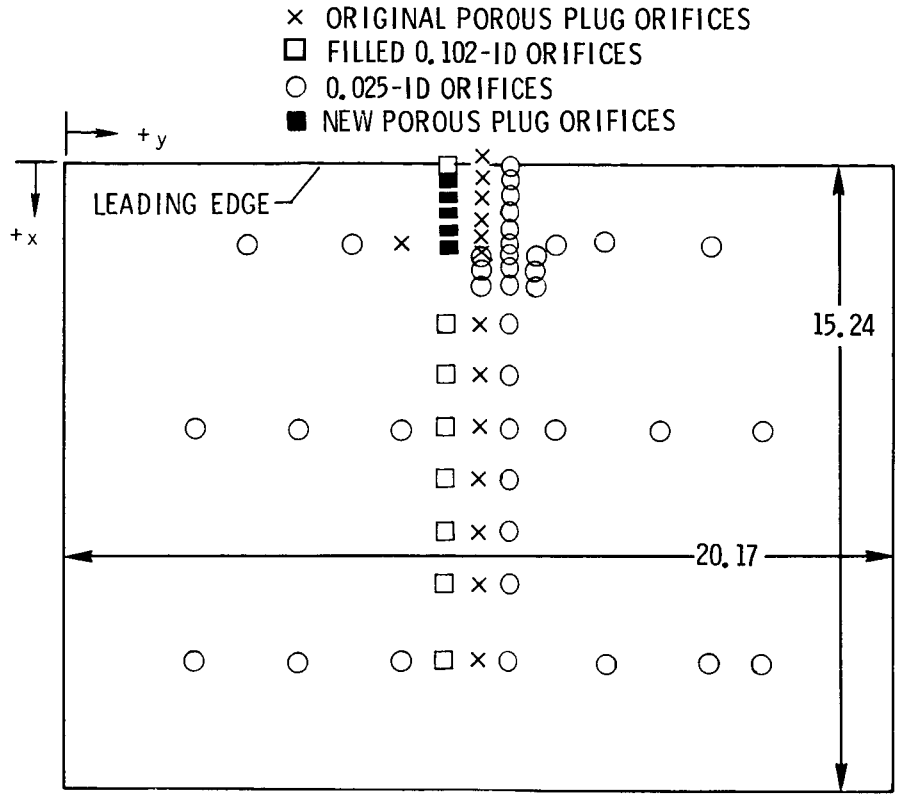

(a) Placement of orifices on upper surface of model. (All dimensions are in centimeters.)

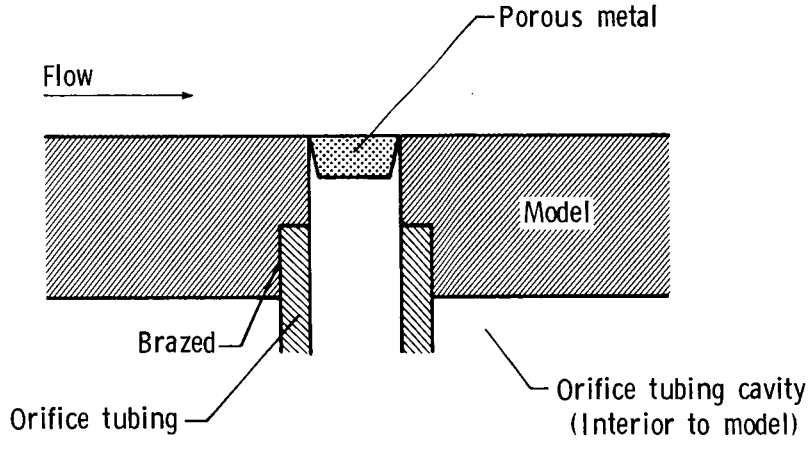

(b) Cross section of porous plug orifice construction for second entry (not drawn to scale).

Figure 6.- Model construction for second tunnel entry.

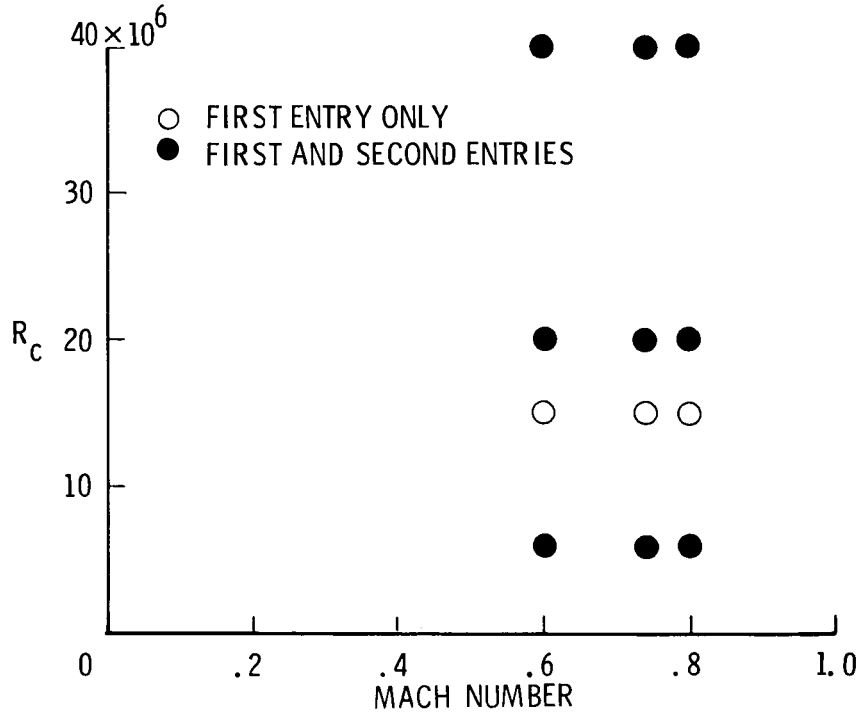

Figure 7.- Reynolds number and Mach number ranges used in test program.

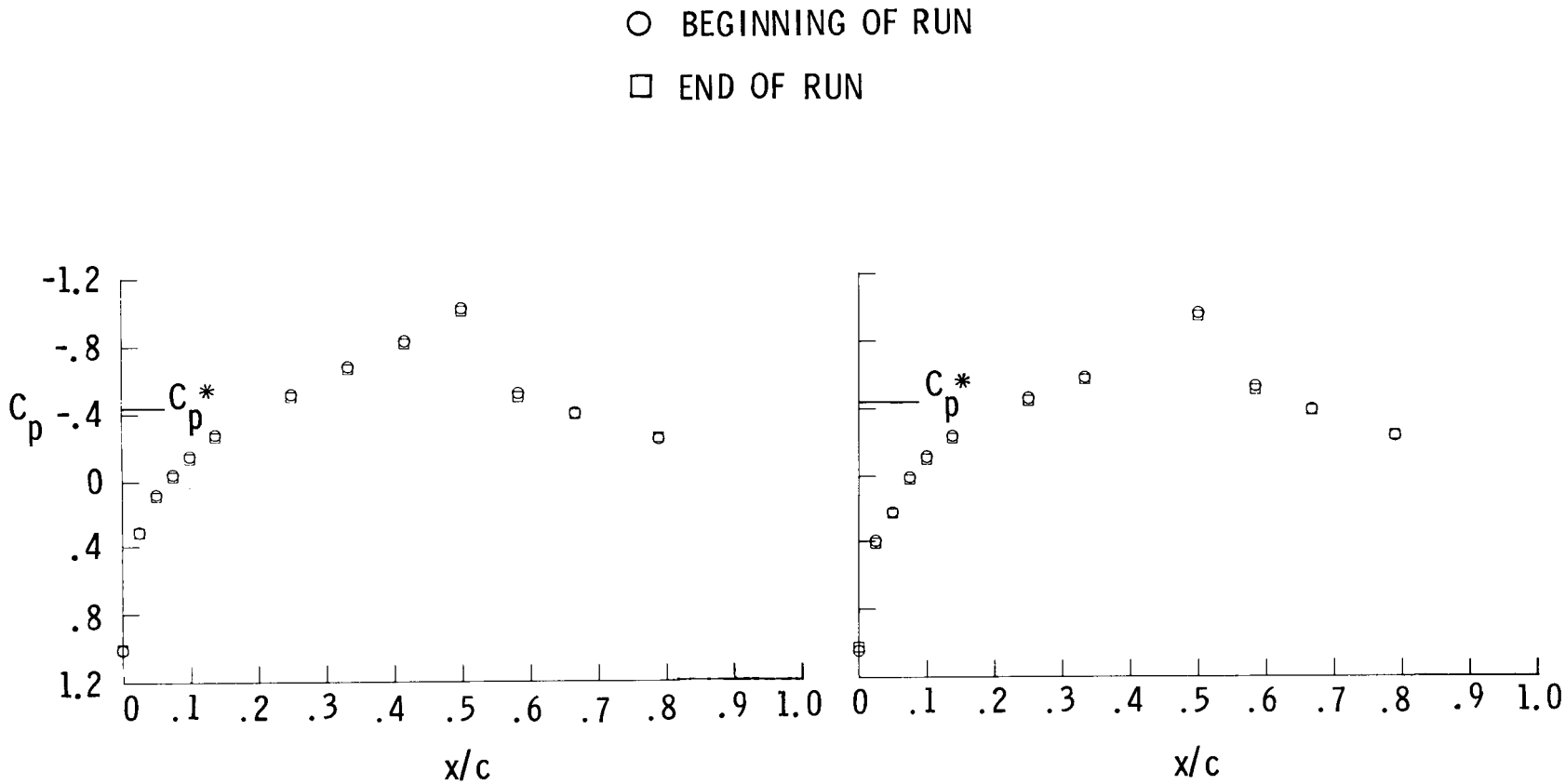

(a) 0.025-cm orifices.

(b) Porous plug orifices.

Figure 8.- Comparison of pressure data from beginning and end of run at $M_\infty = 0.80$, $R_c = 20 \times 10^6$, and $\alpha = 0°$ for first tunnel entry.

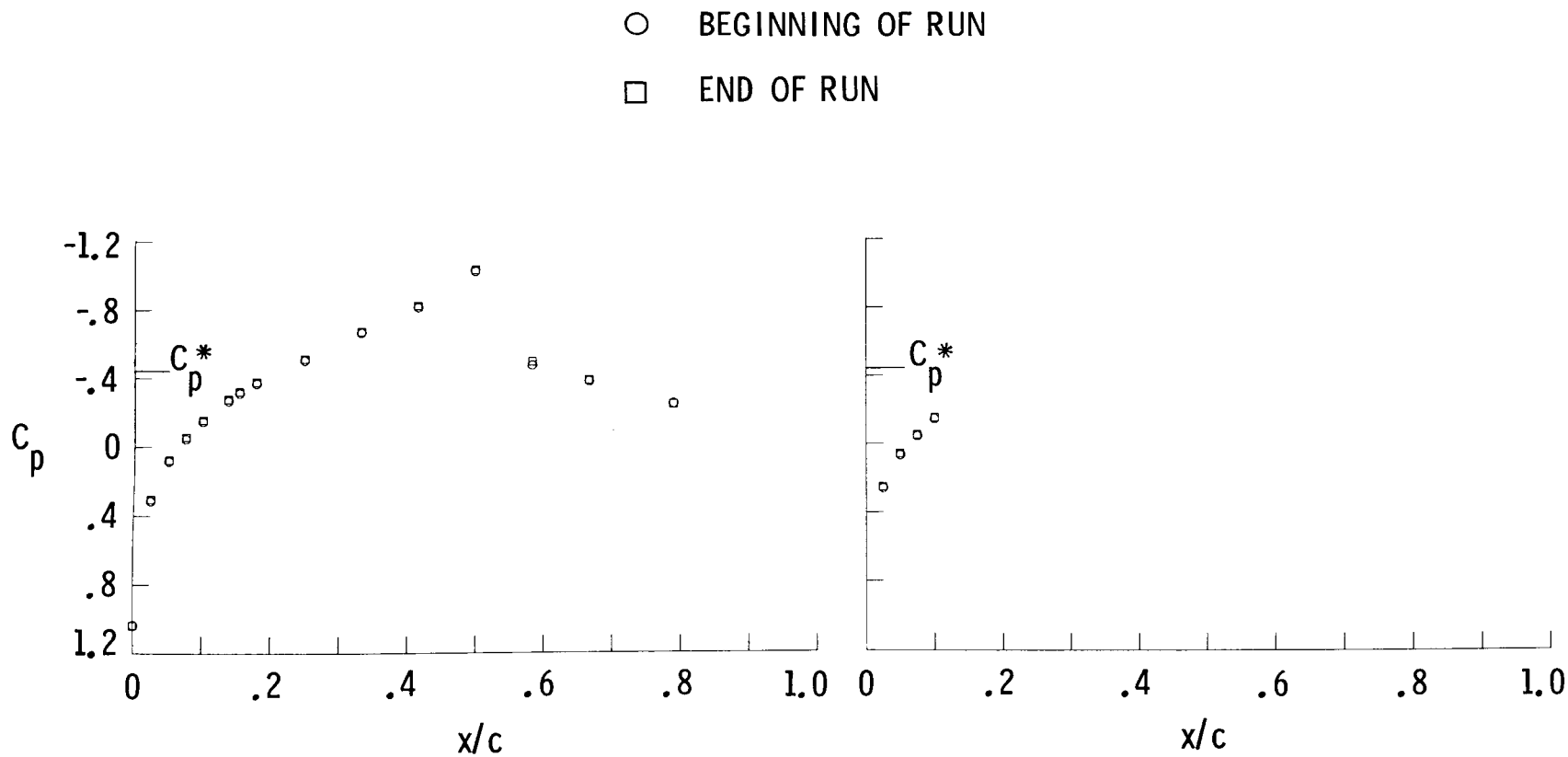

(a) 0.025-cm orifices.

(b) New porous plug orifices.

Figure 9.- Comparison of pressure data from beginning and end of run at $M_\infty = 0.80$, $R_c = 40 \times 10^6$, and $\alpha = 0°$ for second tunnel entry.

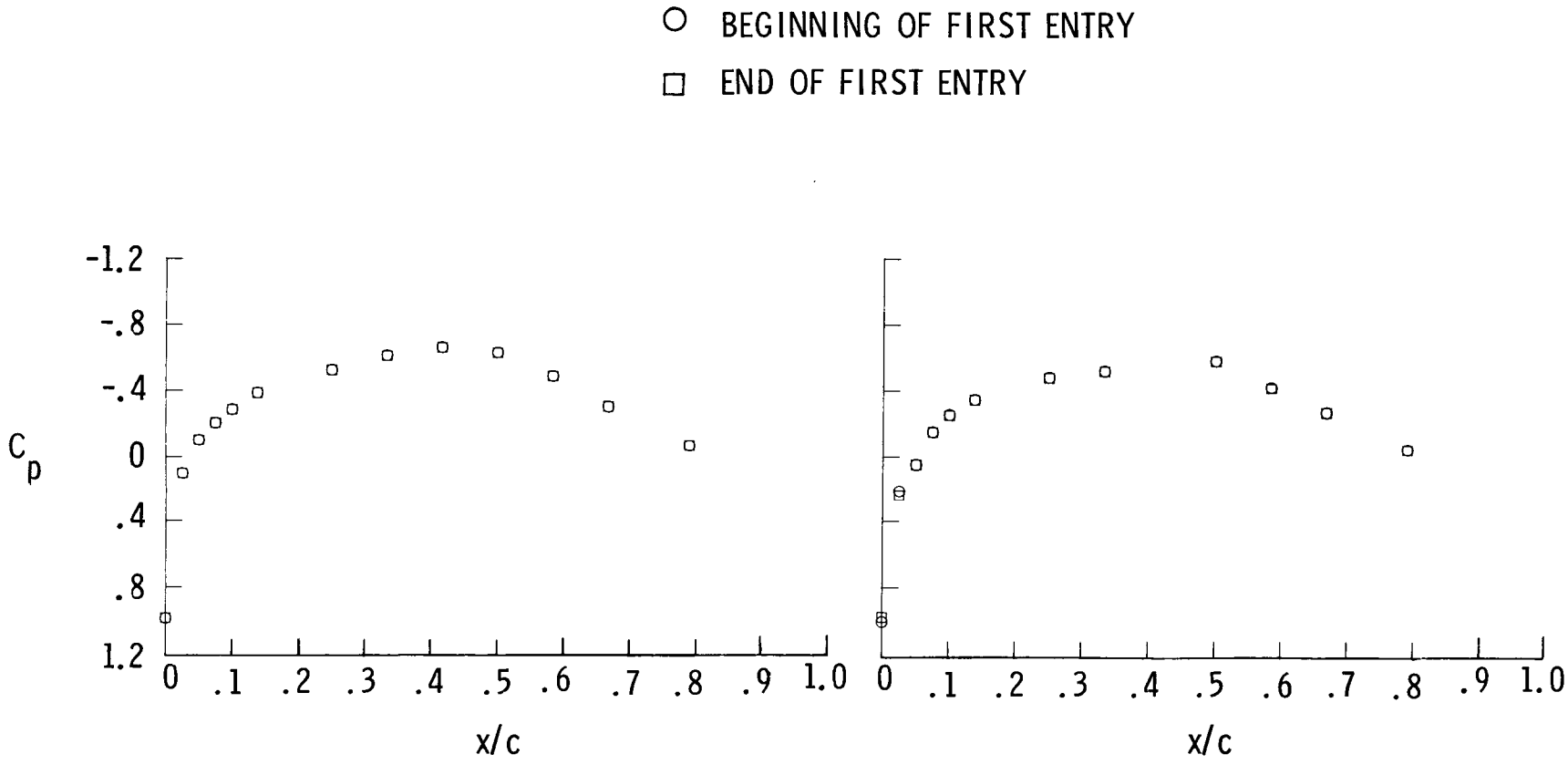

(a) 0.025-cm orifices.

(b) Porous plug orifices.

Figure 10.- Comparison of pressure distribution from beginning and end of test at $M_\infty = 0.60$, $R_c = 15 \times 10^6$, and $\alpha = 0°$.

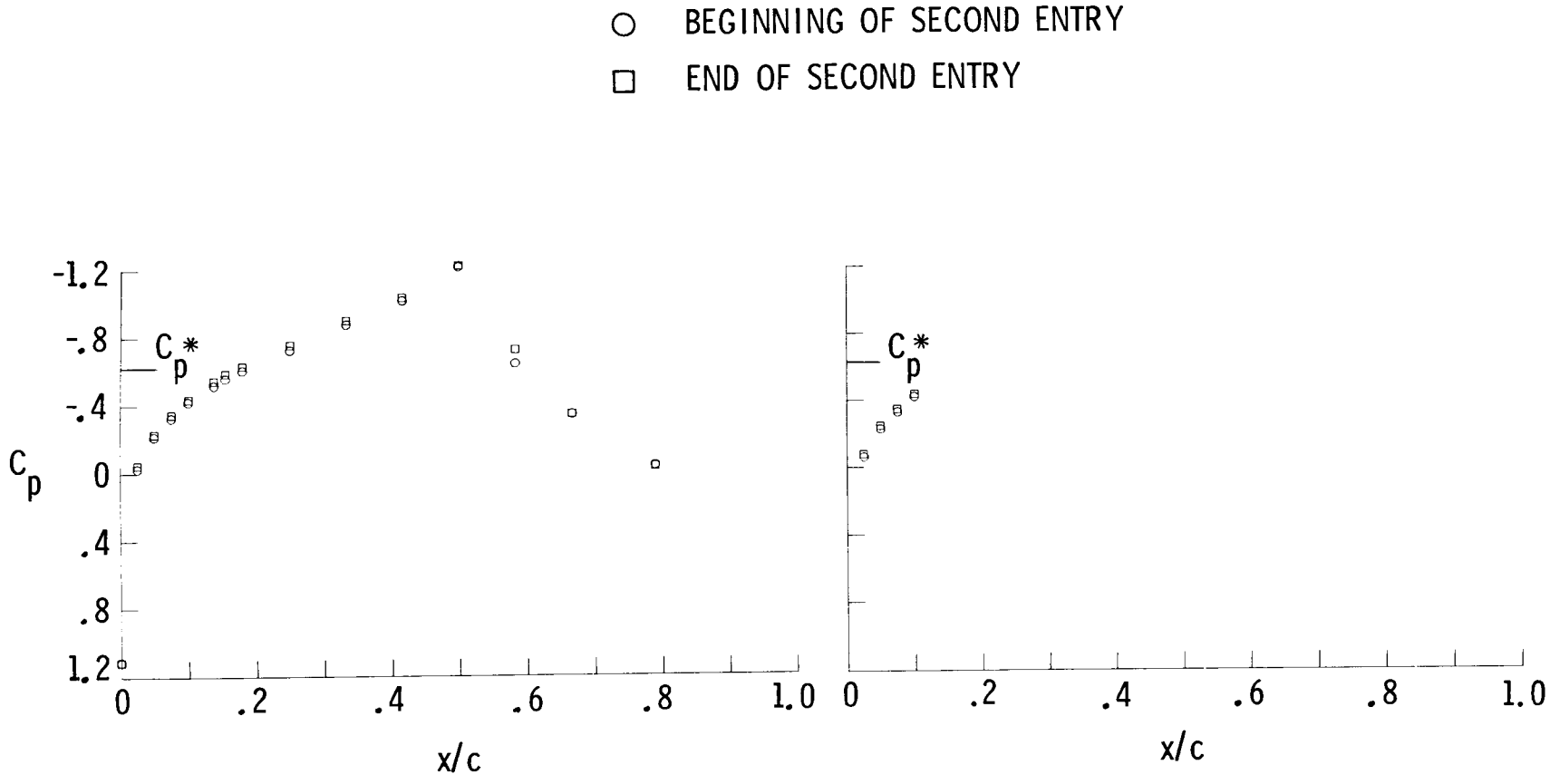

(a) 0.025-cm orifices.

(b) New porous plug orifices.

Figure 11.- Comparison of pressure distributions from beginning and end of second entry at $M_\infty = 0.74$, $R_c = 6 \times 10^6$, and $\alpha = 1°$.

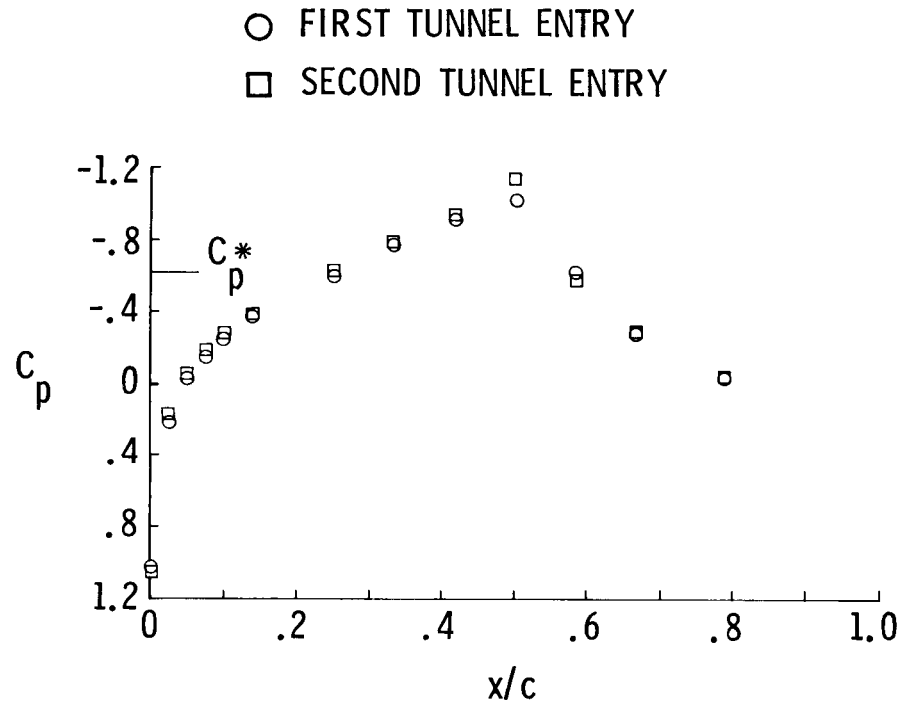

Figure 12.- Comparison of pressure distributions from 0.025-cm orifices for both tunnel entries at $M_\infty = 0.74$, $R_c = 20 \times 10^6$, and $\alpha = 0°$.

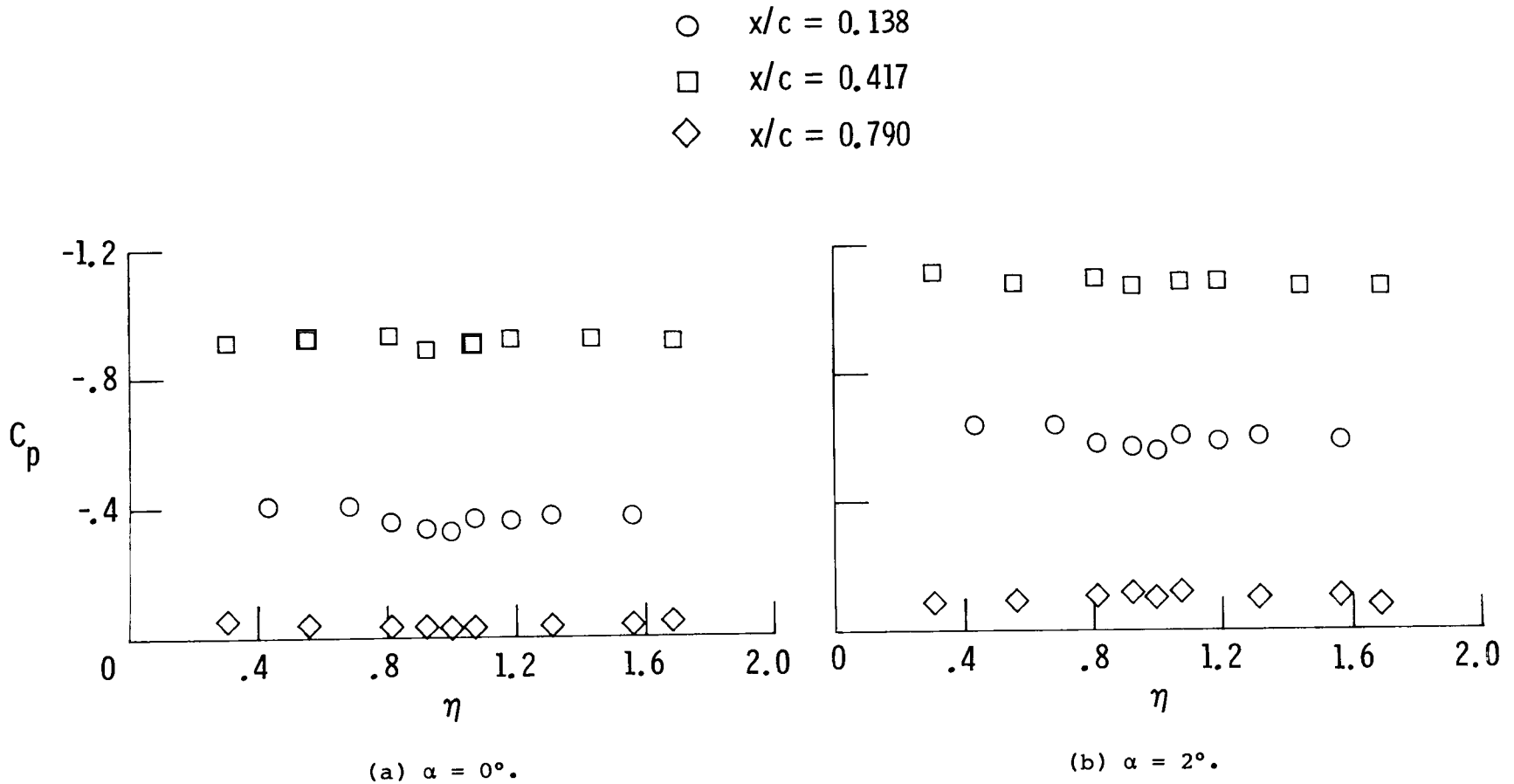

Figure 13.- Spanwise pressures on airfoil from first tunnel entry at $M_\infty = 0.74$ and $R_c = 20 \times 10^6$.

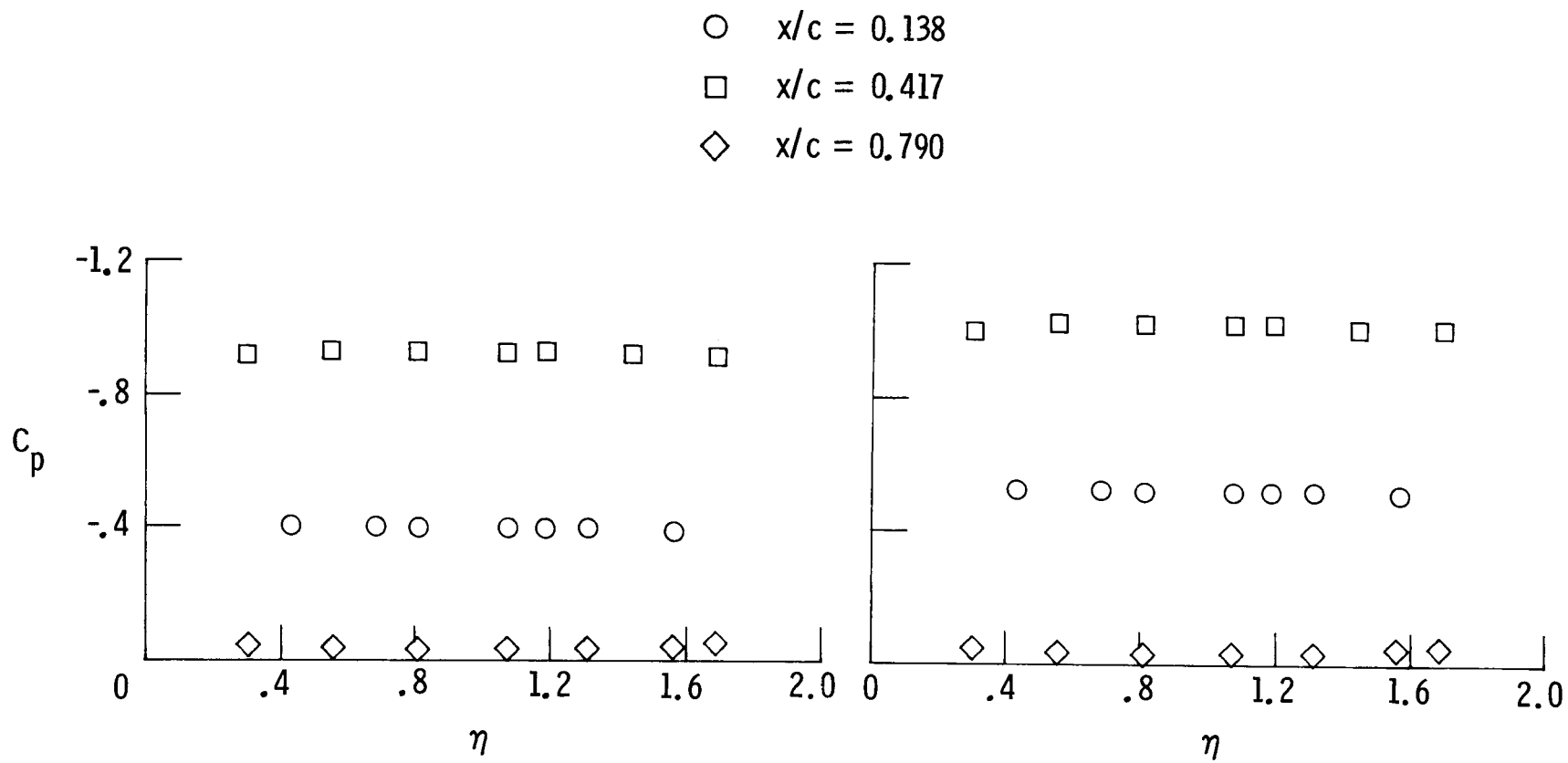

(a) $\alpha = 0°$.

(b) $\alpha = 1°$.

Figure 14.- Spanwise pressures on airfoil from second tunnel entry at $M_\infty = 0.74$ and $R_c = 20 \times 10^6$.

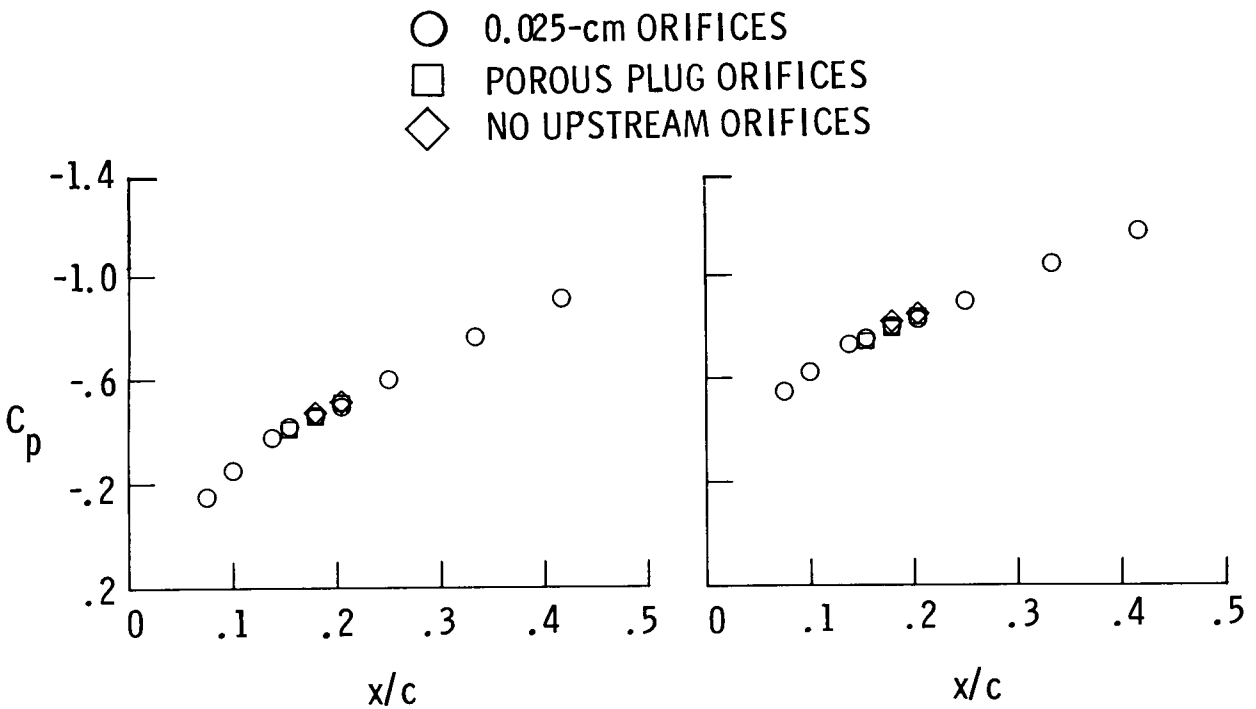

(a) $\alpha = 0°$.

(b) $\alpha = 3°$.

Figure 15.- Downstream effect of orifices at $M_\infty = 0.74$ and $R_c = 15 \times 10^6$.

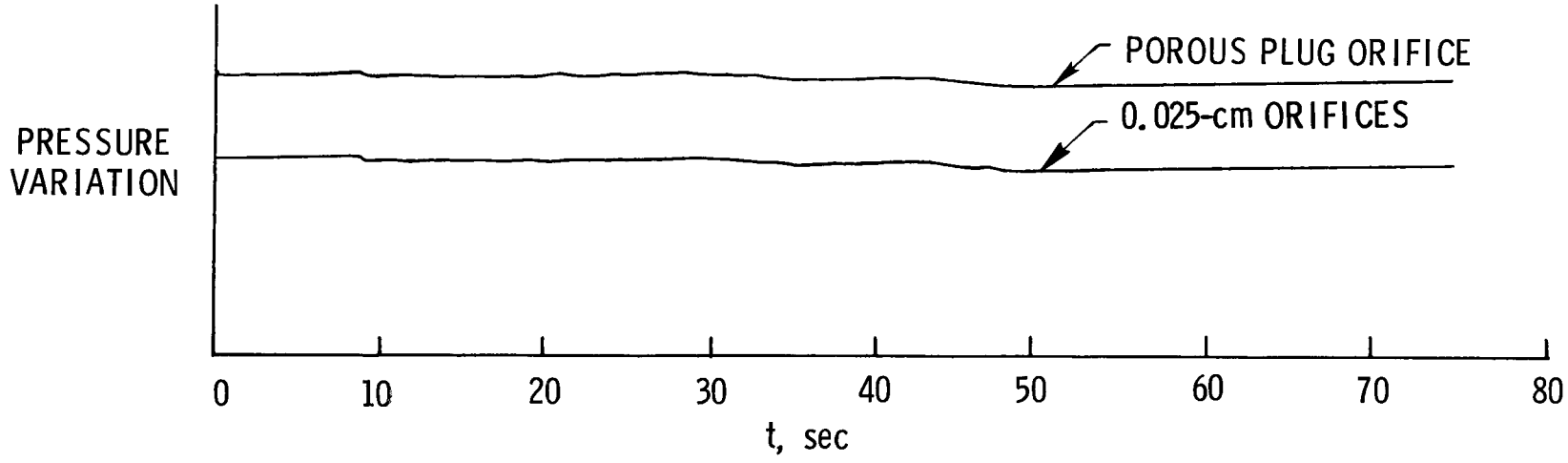

(a) x/c = 0.025.

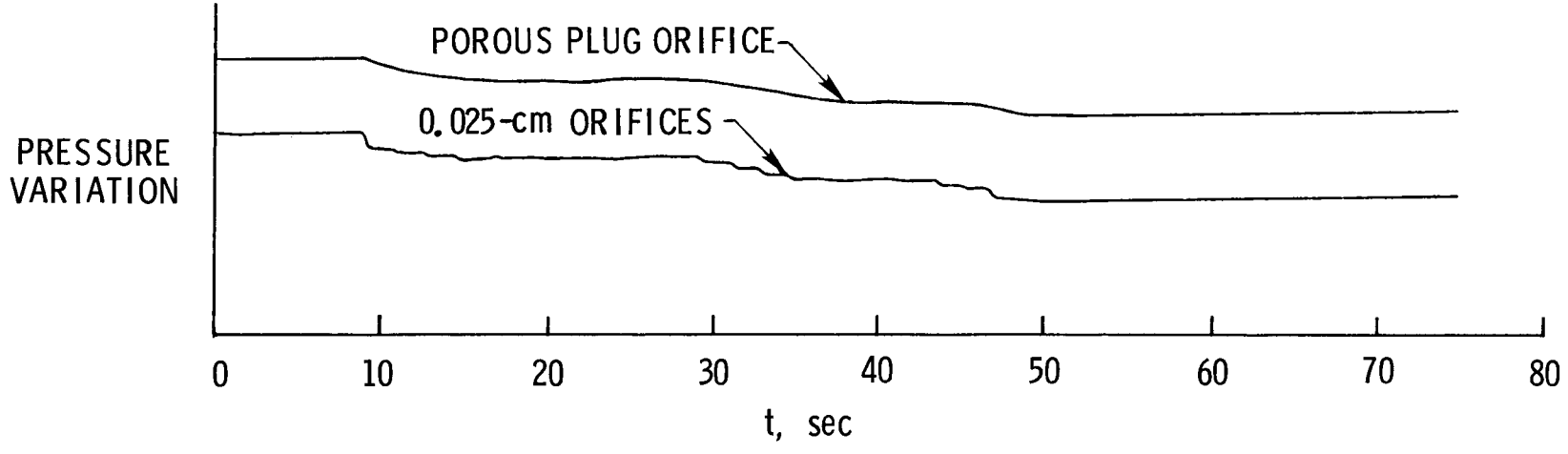

(b) x/c = 0.417.

Figure 16.- Oscillograph comparison of response times at $M_\infty = 0.60$ and $R_c = 15 \times 10^6$.

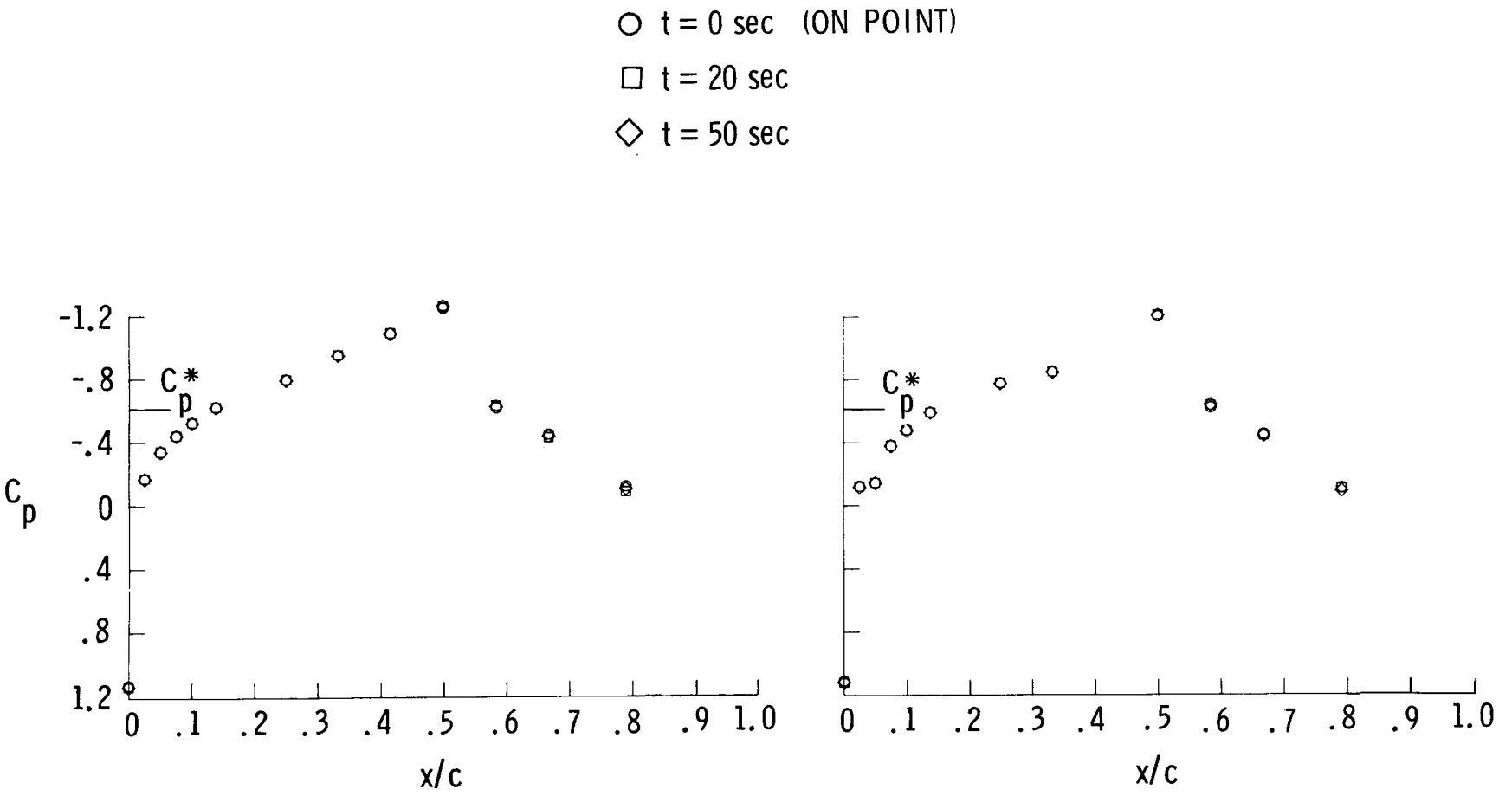

(a) 0.025-cm orifices.

(b) Porous plug orifices.

Figure 17.- Comparison of pressures at several time intervals at $M_\infty = 0.74$, $R_C = 6 \times 10^6$, and $\alpha = 2°$.

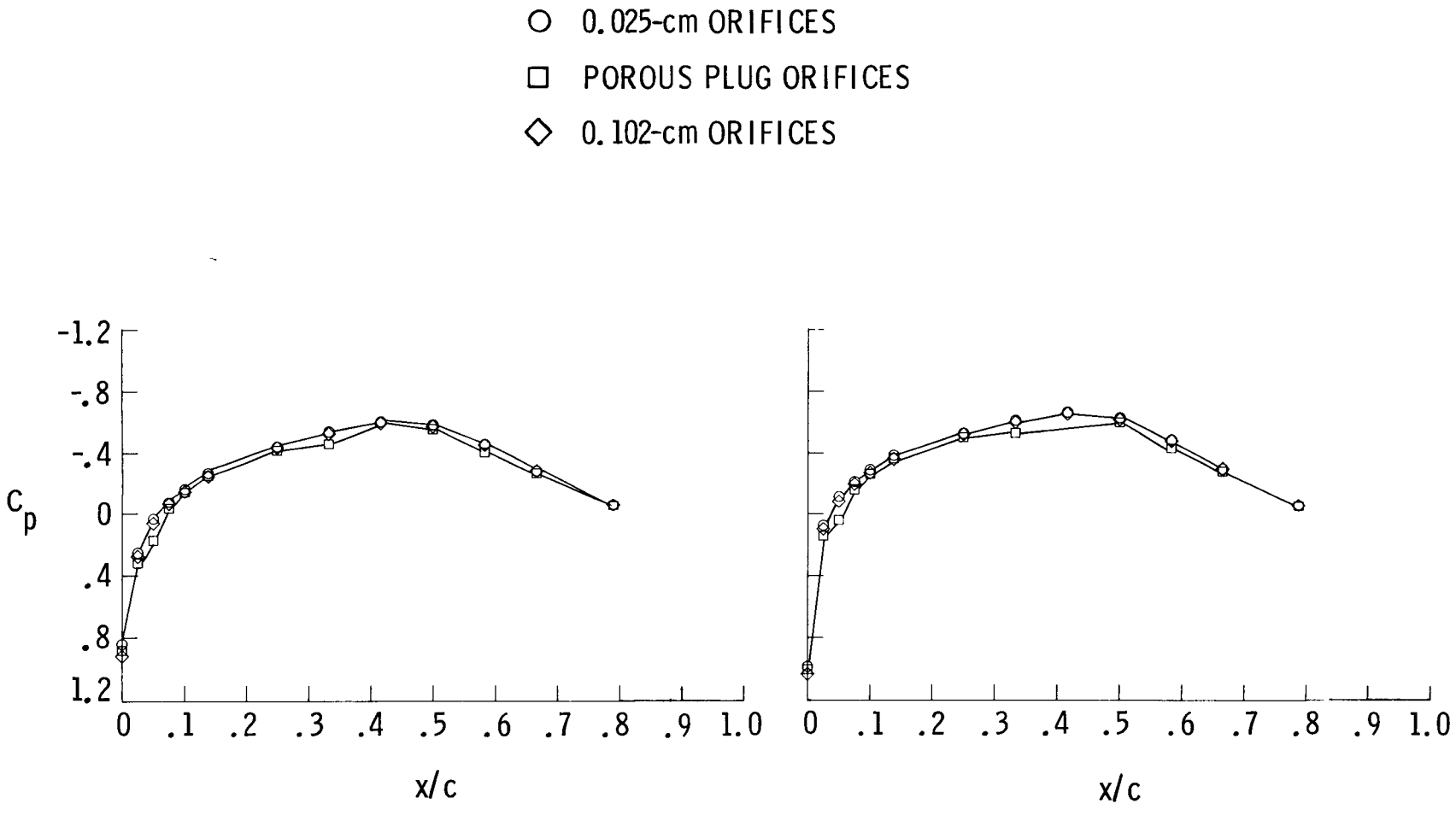

(a) $\alpha = -1°$.

(b) $\alpha = 0°$.

Figure 18.- Effect of orifice size on pressure distribution in first tunnel entry at $M_\infty = 0.60$ and $R_c = 6 \times 10^6$.

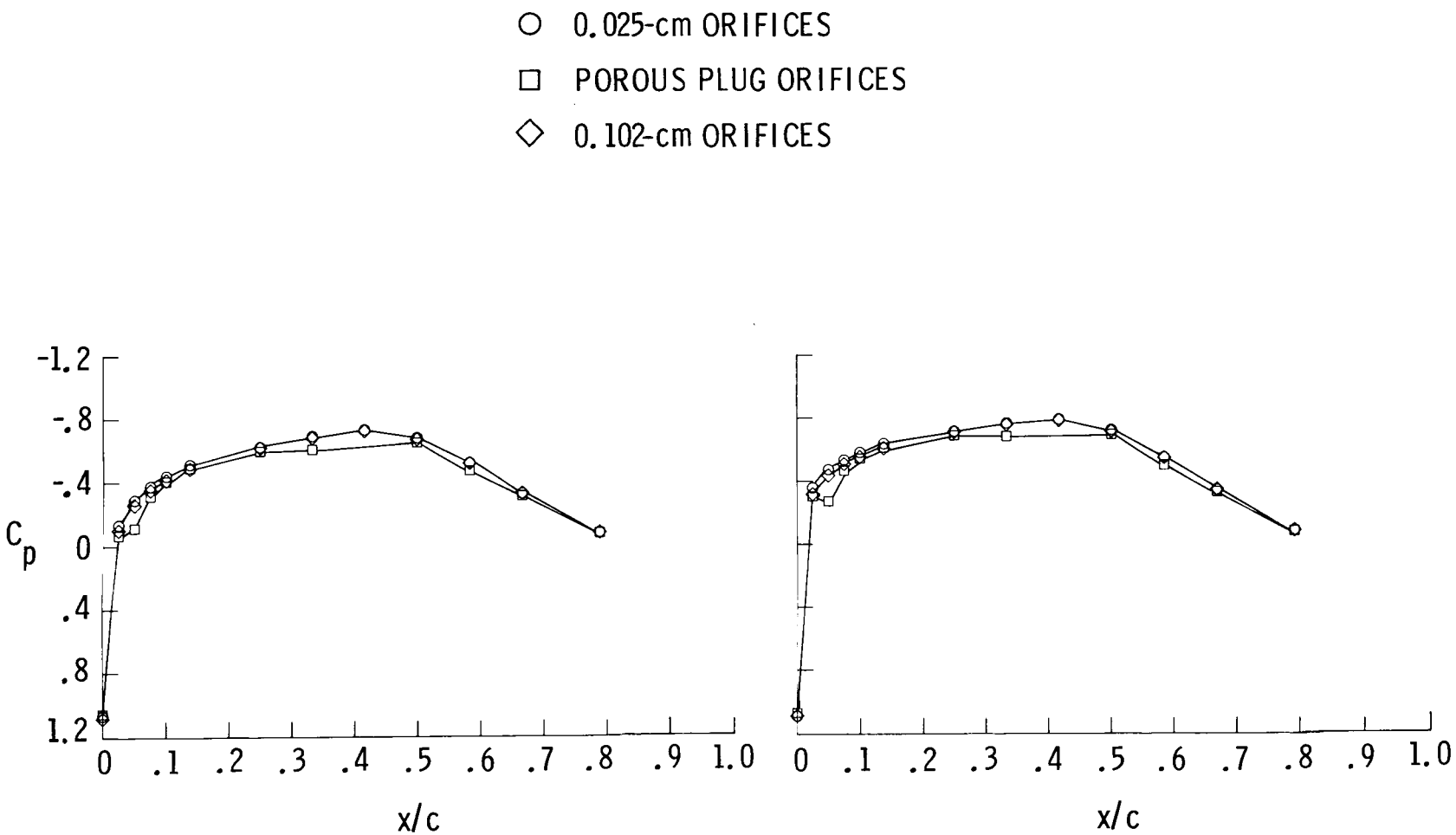

(c) $\alpha = 1°$.

(d) $\alpha = 2°$.

Figure 18.- Continued.

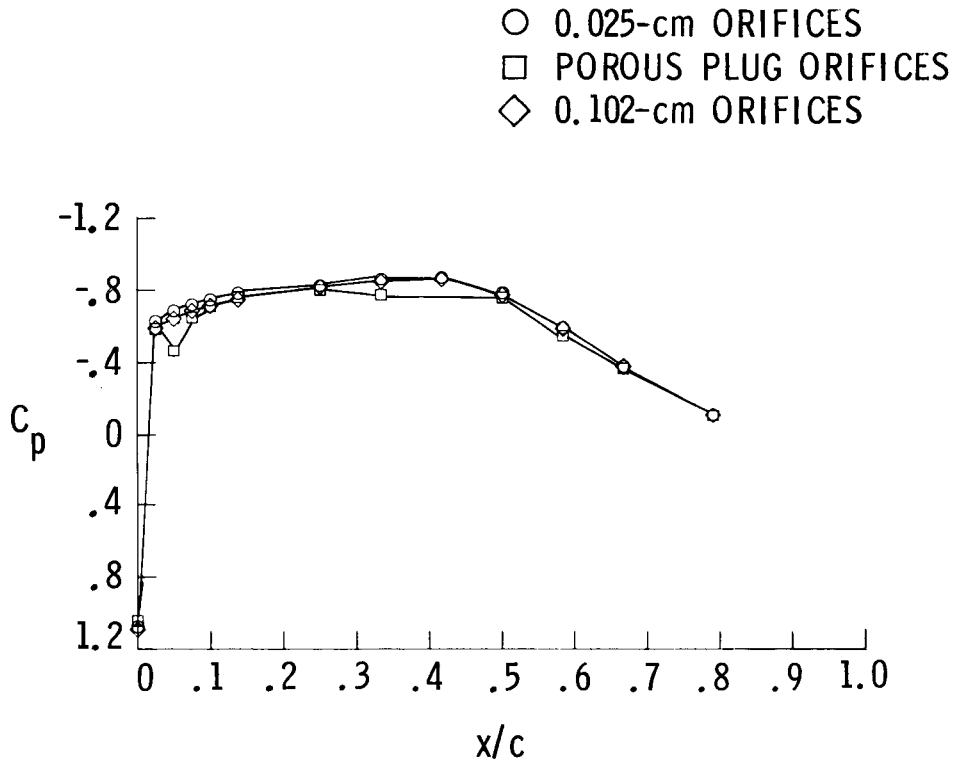

(e) $\alpha = 3°$.

Figure 18.- Concluded.

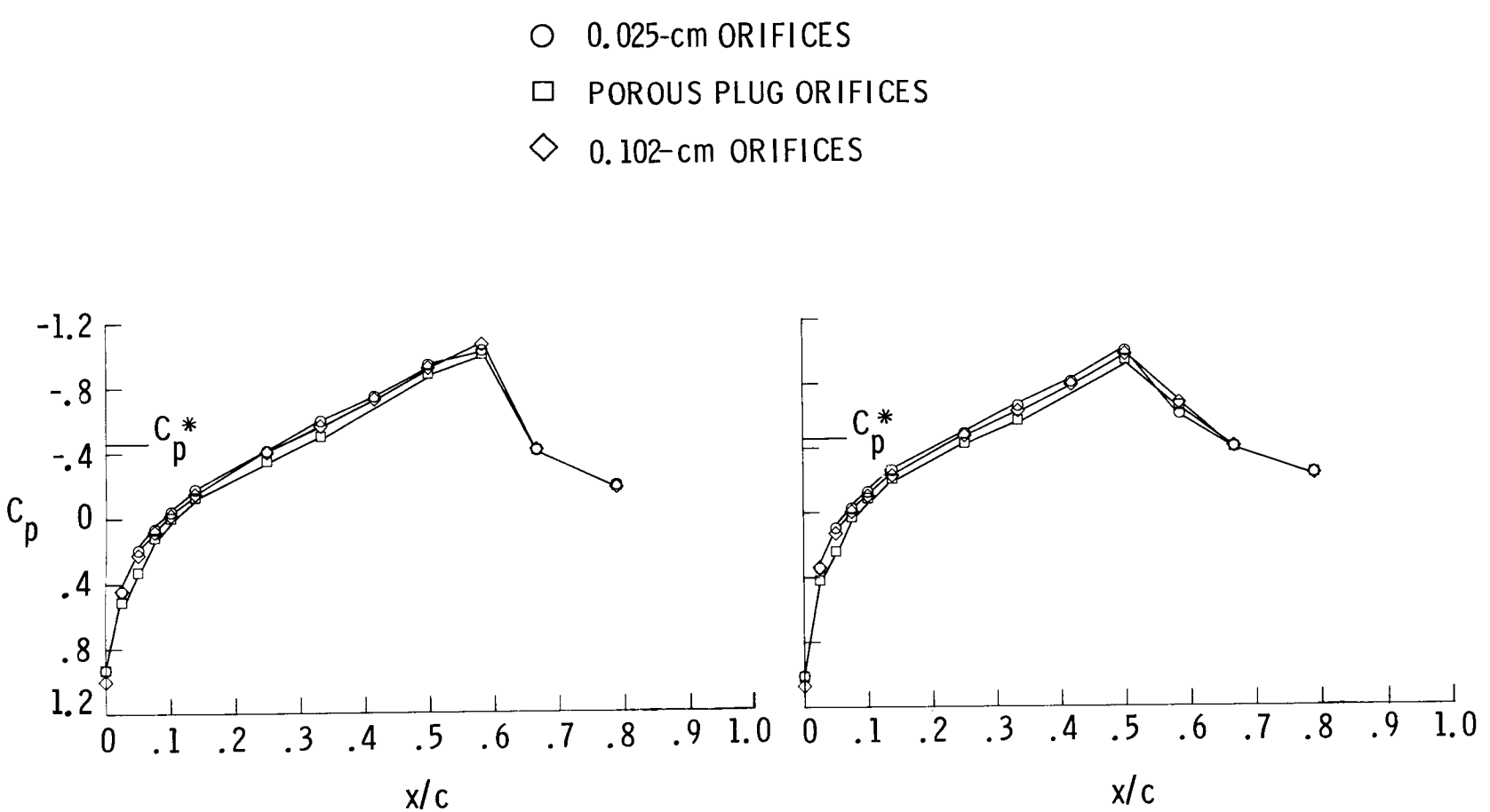

(a) $\alpha = -1°$.

(b) $\alpha = 0°$.

Figure 19.- Effect of orifice size on pressure distribution in first tunnel entry at $M_\infty = 0.80$ and $R_c = 40 \times 10^6$.

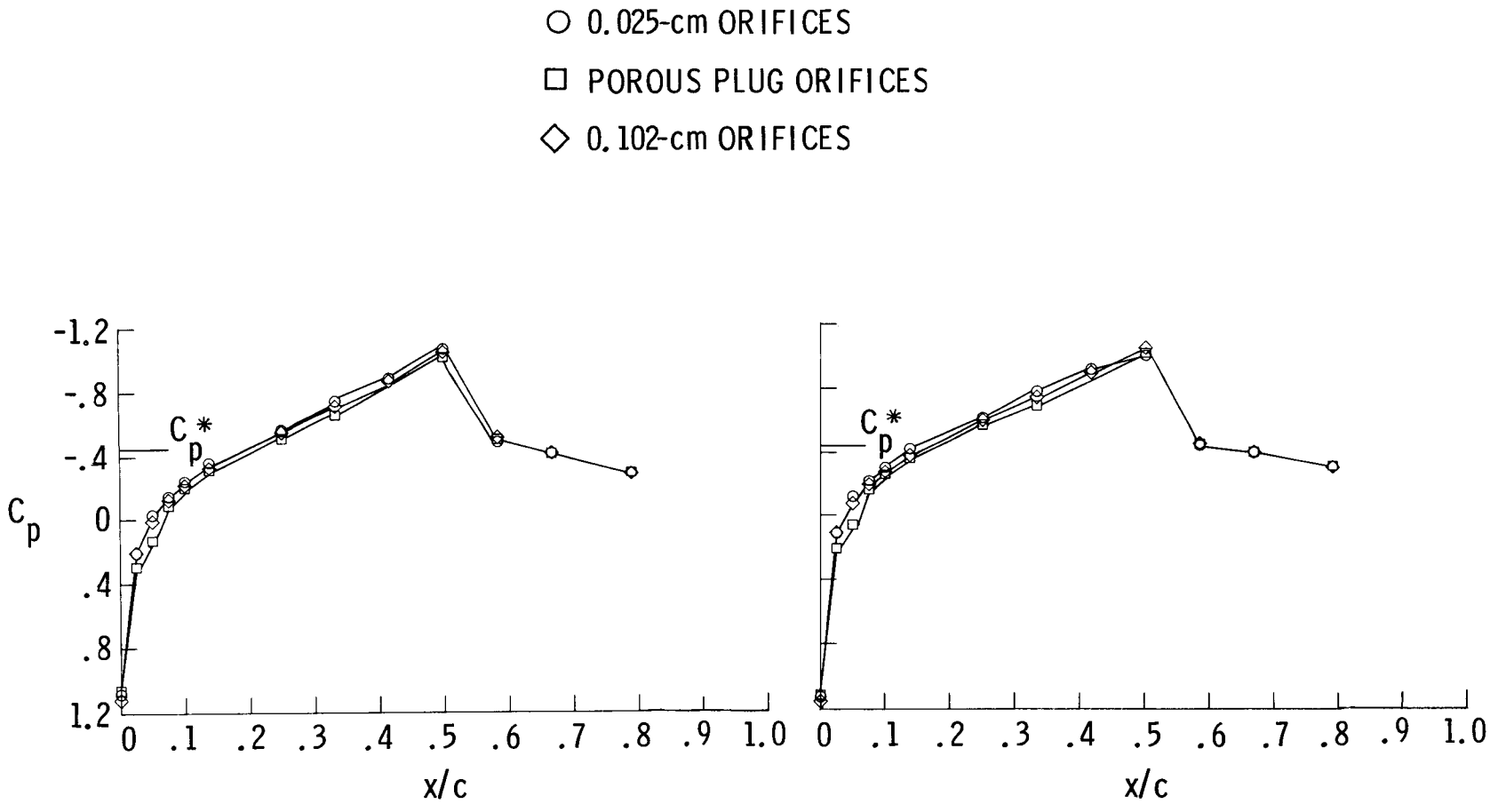

(c) $\alpha = 1°$.

(d) $\alpha = 2°$.

Figure 19.- Concluded.

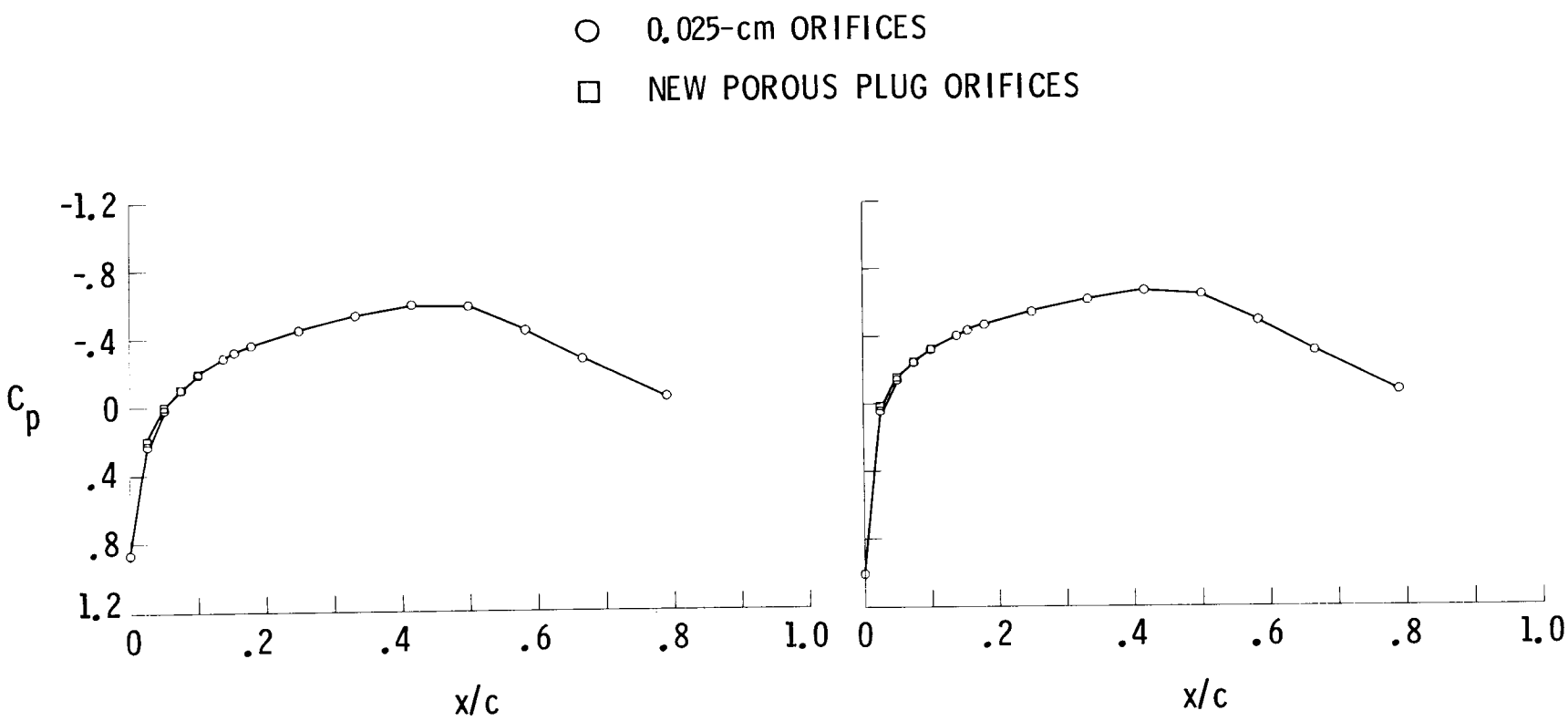

Figure 20.- Effect of orifice on pressure distribution in second tunnel entry at $M_\infty = 0.60$ and $R_c = 6 \times 10^6$.

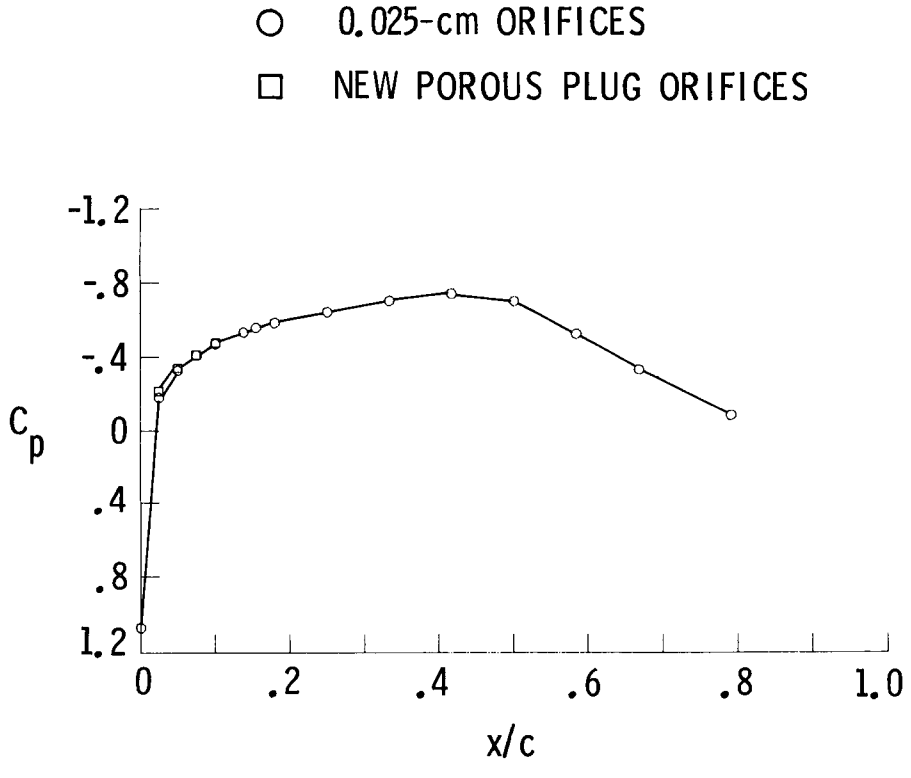

(c) $\alpha = 1°$.

Figure 20.- Concluded.

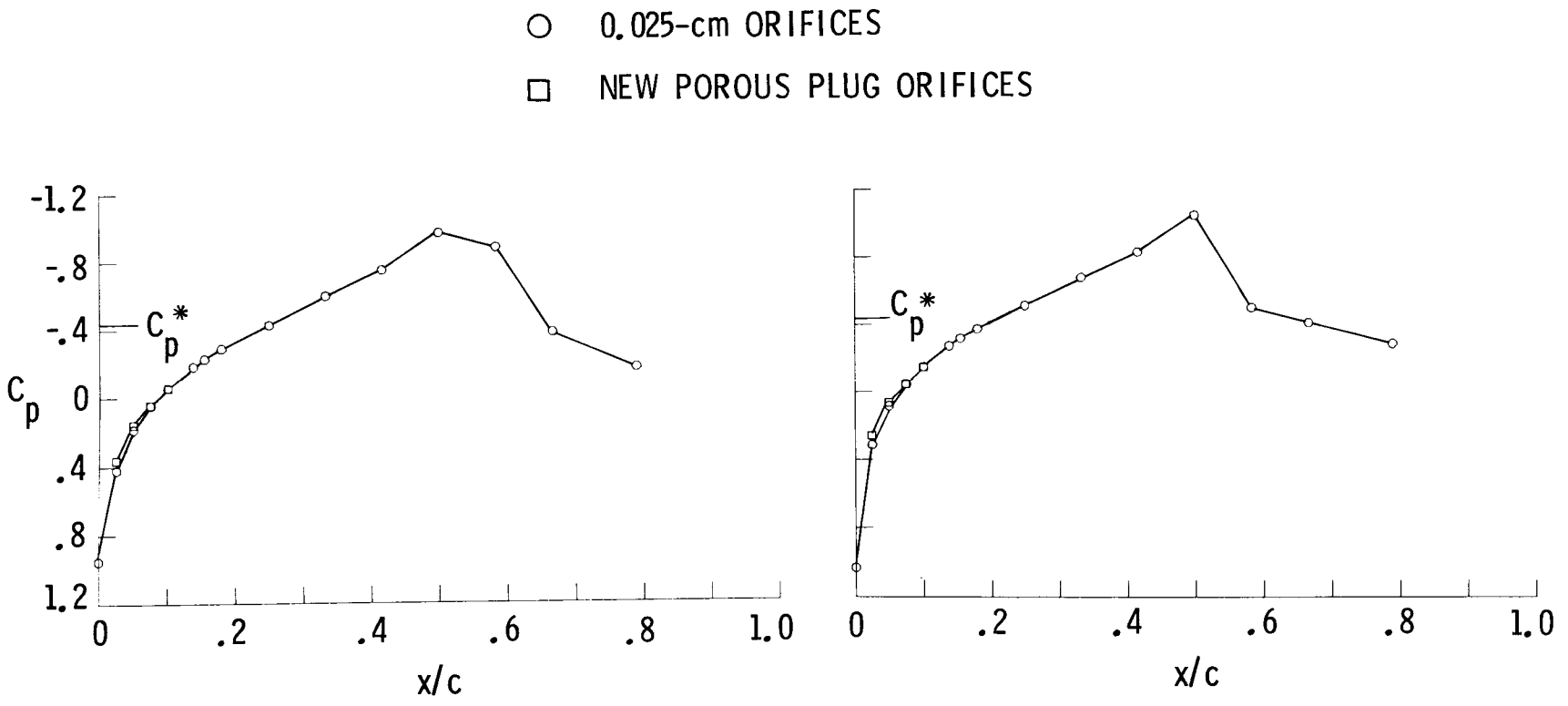

(a) $\alpha = -1°$.

(b) $\alpha = 0°$.

Figure 21.- Effect of orifice on pressure distribution in second tunnel entry at $M_\infty = 0.80$ and $R_c = 40 \times 10^6$.

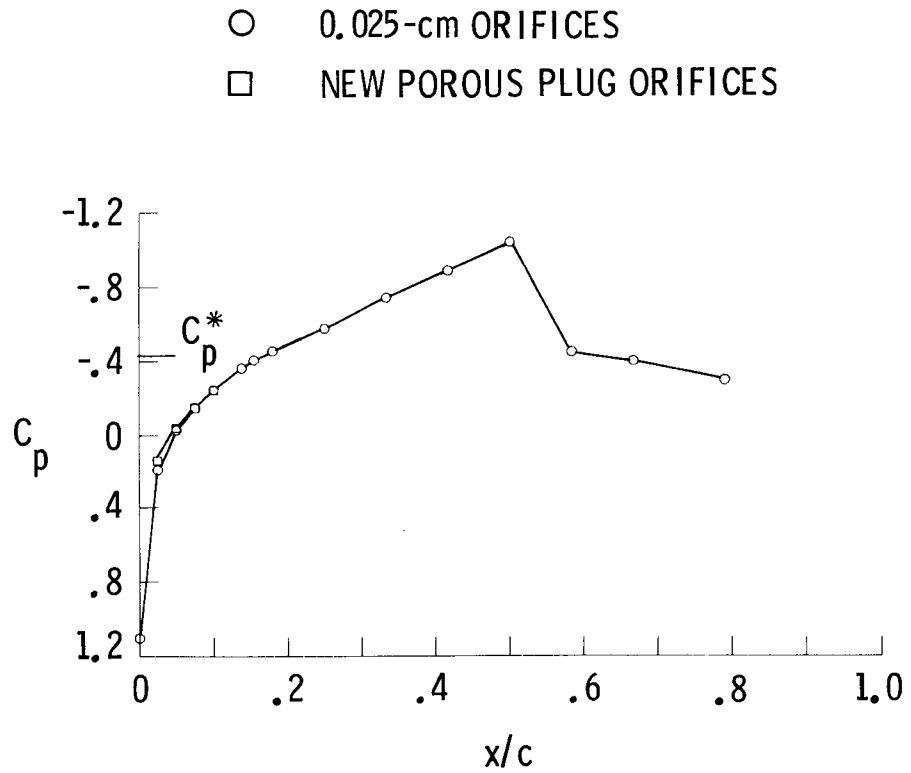

(c) $\alpha = 1°$.

Figure 21.- Concluded.

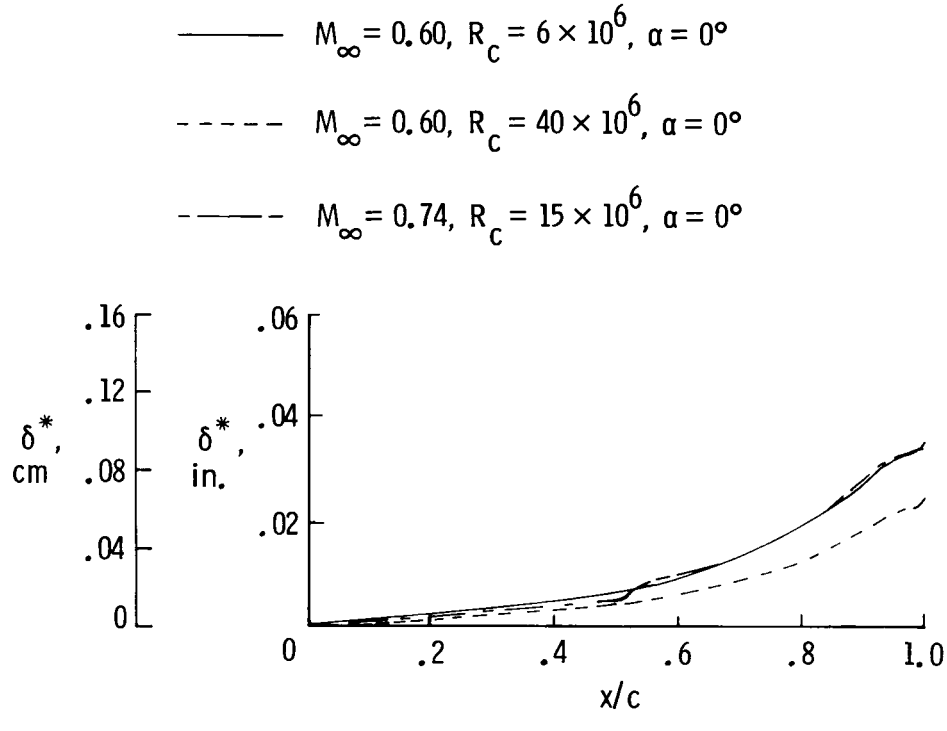

Figure 22.- GRUMFOIL-calculated values of δ^* versus x/c for turbulent boundary layer.

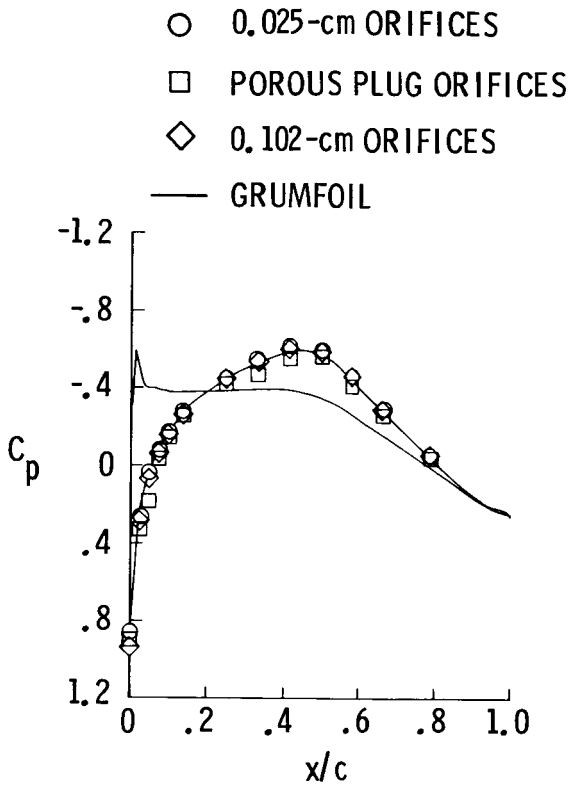

(a) $\alpha = -1°$.

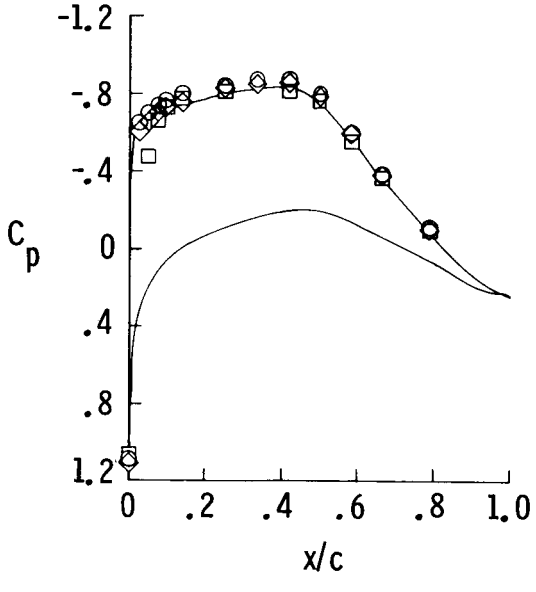

(b) $\alpha = 3°$.

Figure 23.- Comparison of GRUMFOIL-generated pressure distributions with first-entry data at $M_\infty = 0.60$ and $R_c = 6 \times 10^6$.

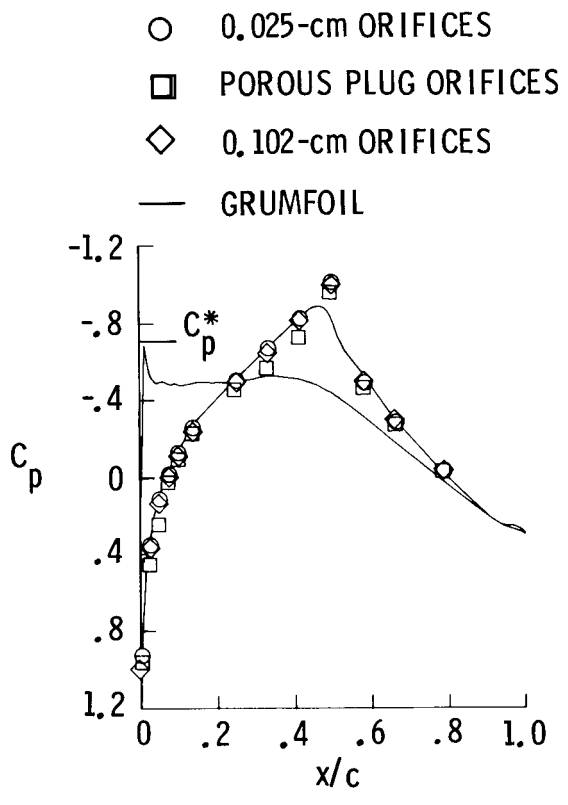

(a) $\alpha = -1°$.

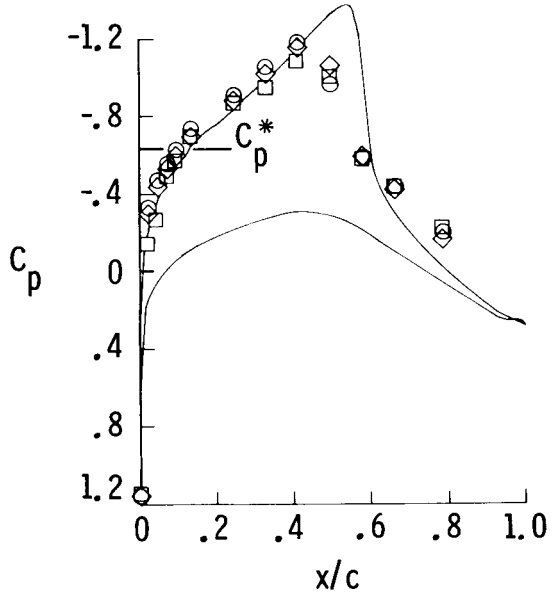

(b) $\alpha = 3°$.

Figure 24.- Comparison of GRUMFOIL-generated pressure distributions with first-entry data at $M_\infty = 0.74$ and $R_c = 15 \times 10^6$.

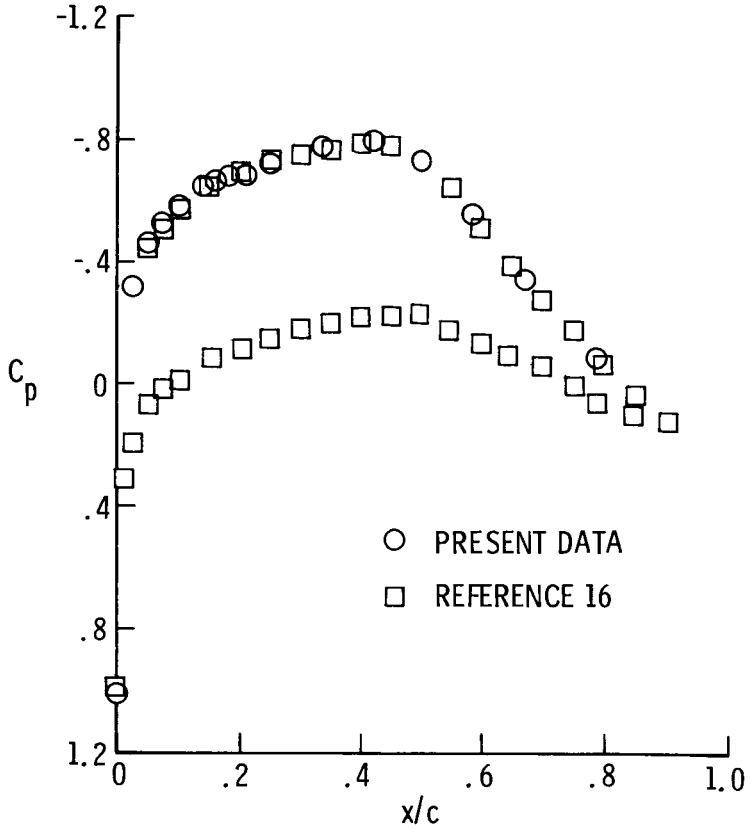

Figure 25.- Comparison of pressure data on 0.025-cm orifice from first tunnel entry with data from reference 16. $M_\infty = 0.60$; $R_c = 20 \times 10^6$; $\alpha = 2°$.

1. Report No.	2. Government Accession No.	3. Recipient's Catalog No.
NASA TP-2537		

4. Title and Subtitle	5. Report Date
The Application to Airfoils of a Technique for Reducing Orifice-Induced Pressure Error at High Reynolds Numbers	January 1986
	6. Performing Organization Code 505-31-23-07
7. Author(s) E. B. Plentovich	8. Performing Organization Report No. L-16002
	10. Work Unit No.
9. Performing Organization Name and Address NASA Langley Research Center Hampton, VA 23665-5225	11. Contract or Grant No.
	13. Type of Report and Period Covered Technical Paper
12. Sponsoring Agency Name and Address National Aeronautics and Space Administration Washington, DC 20546-0001	14. Sponsoring Agency Code

15. Supplementary Notes

16. Abstract

A wind-tunnel investigation was conducted in the Langley 0.3-Meter Transonic Cryogenic Tunnel to study the effects of porous (sintered metal) plug orifices on orifice-induced static-pressure measurement error at high Reynolds numbers. An NACA 65_1-213 airfoil was tested at Mach numbers from 0.60 to 0.80 and at Reynolds numbers from 6×10^6 to 40×10^6. Data are included which compare pressure measurements obtained from porous plug orifices and from conventional orifices with diameters of 0.025 cm (0.010 in.) and 0.102 cm (0.040 in.). The two-dimensional airfoil code GRUMFOIL was used to calculate boundary-layer displacement thickness. The response time and the downstream effect of the porous plug orifice were considered in this investigation. The results showed that the porous plug orifice could be a viable method of reducing pressure error. The data also showed that the pressure measurements obtained with a 0.102-cm-diameter orifice were very close to the measurements obtained with a 0.025-cm-diameter orifice over much of the airfoil and that downstream of a shock the orifice size was not critical.

17. Key Words (Suggested by Author(s))		18. Distribution Statement
Pressure measurement	Transonic flow	Unclassified - Unlimited
Static pressure	Cryogenic wind tunnels	
Orifices	Airfoils	
Errors		
Porous materials		Subject Category 02

19. Security Classif. (of this report)	20. Security Classif. (of this page)	21. No. of Pages	22. Price
Unclassified	Unclassified	42	A03

For sale by the National Technical Information Service, Springfield, Virginia 22161

NASA-Langley, 1986